# Seismic Risk Assessment of Actively Controlled Buildings under Probable Mainshock-Aftershock Scenarios during their Lifetime

**Ali Khansefid**
KN Toosi University of Technology
**Ali Bakhshi** ( bakhshi@sharif.edu )
Sharif University of Technology https://orcid.org/0000-0003-0001-8326

**Research Article**

**Keywords:** Active Control, Life-Cycle Cost, Lifetime Seismic Risk, LQR Algorithm, Mainshock-Aftershock Sequence, Monte-Carlo Simulation, Multi-Objective Optimization.

**Posted Date:** April 8th, 2021

**DOI:** https://doi.org/10.21203/rs.3.rs-398977/v1

# Seismic Risk Assessment of Actively Controlled Buildings under Probable Mainshock-Aftershock Scenarios during their Lifetime

**A. Khansefid[1], A. Bakhshi[2]**

1- Department of Civil Engineering, KN Toosi University of Technology, Tehran, Iran

2- Department of Civil Engineering, Sharif University of Technology, Tehran, Iran

Corresponding Author Email: Bakhshi@sharif.edu

**ABSTRACT**

This paper focuses on a new comprehensive probabilistic approach for lifetime risk assessment of buildings equipped with active vibration control systems under future probable mainshock-aftershock scenarios. This procedure starts from the seismic hazard simulation, continues with the building performance evaluation, and ends with the seismic risk assessment. The procedure attempts to reflect the effects of major uncertainty sources existing in both building properties and earthquake scenarios using the Monte-Carlo simulation technique. The method is applied to steel moment-resisting frame buildings armed with the optimally designed active vibration control system (using the linear quadratic regulator algorithm). In each realization of the Monte-Carlo simulation, first, a random earthquake scenario containing probable future mainshock-aftershock sequences and their corresponding synthetic stochastic accelerograms are procreated. Next, the buildings are designed in two separate cases, with and without the presence of active vibration control systems. The former is designed based on the international design codes, while the latter properties are obtained via an advanced optimization method. In the last step, considering all generated samples, the loss curve of buildings with the active control system is developed for two separate cases: with or without taking aftershocks' effects into account. The application of this method indicates that the active control system works well in decreasing the loss value (on average 66%) of buildings during their 50-year lifetime, especially in the more intensive earthquake scenarios. Additionally, it is shown that by neglecting the aftershocks, the life-cycle cost of building will be estimated tangibly (on average 70%) less than what it would be. Finally, it is observed that the non-structural acceleration-sensitive damages have a higher contribution in total building losses in uncontrolled structures in comparison with the actively controlled building by considering aftershocks.

**Keywords:**

Active Control; Life-Cycle Cost; Lifetime Seismic Risk; LQR Algorithm; Mainshock-Aftershock Sequence; Monte-Carlo Simulation; Multi-Objective Optimization.

## 1. INTRODUCTION

The application of vibration control systems in some projects is faced some kind of resistance by their owners due to their initial cost. However, their technical supremacy to the traditional structural systems is accepted. This challenge is mostly due to the inappropriate perspective about all costs of a building during its lifetime. Where the most of existing well-known building design provisions (BHRC 2014, ASCE 2016, European Committee for Standardization 2004) remain silent. In recent decades, ongoing efforts have been launched to propose approaches for designing buildings considering the desired performance level (Gibson 1982, Yamawaki et al. 2000, Liu et al. 2004, Becker 2008). However, this is not adequate, and it is required to step forward through the methodologies, which can give some insights to the owners about the probable future damages and losses of their building. This is exactly the main target of this research by developing a comprehensive methodology starting from hazard modeling, continuing by calculating structural response and estimating the damage levels, and ends with evaluating the lifetime risk.

In general, by reviewing the previous research works, a number of studies can be found on the probabilistic design and life-cycle cost assessment of buildings during their life span (Lagaros 2007, Mitropoulou et al. 2011, Loli et al. 2017, Rabonza and Lallemant, 2019, Noureldin and Kim 2021), even when they are equipped with vibration control systems. As an early work, Wen and Shinozuka (1997) tried to evaluate the cost of structures equipped with active vibration control systems by the Incremental Dynamic Analysis. Park et al. (2004) introduced a life-cycle-based minimization procedure to design the viscoelastically damped structures. Dogruel (2009) did a life-cycle cost-benefit analysis for retrofitting buildings with passive control devices, including metallic damper, viscous fluid damper, and viscoelastic damper. Dang et al. (2015) worked on the performance assessment of base isolation systems using the life-cycle-based approach. Gidaris and Taflanidis (2012, 2015) presented a probabilistic approach for the life-cycle-cost-based design of viscous dampers for seismic hazards.

Hahm et al. (2013) proposed a methodology to assess the life-cycle cost of a state-cable bridge equipped with magnetorheological dampers. Mitropoulou et al. (2016) worked on the optimization of life-cycle cost of base isolation systems. Ruize et al. (2016) dealt with the design of mass dampers in accordance with their life-cycle cost. Micheli (2017) attempted to present a probabilistic framework for designing high-performance control systems like semi-active and active devices. Park et al. (2017) developed a new methodology for the design of viscoelastically damped structures based on their life-cycle cost. Scozzesea et al. (2019) evaluated the sensitivity of estimated seismic risk of structures equipped with the fluid viscous dampers to their properties. More recently, Shi et al. (2020) assessed the capability of shape memory alloy dampers in reducing the seismic risk under mainshocks and aftershocks.

In this research, an attempt is made to propose a methodology for evaluating the lifetime seismic risk of buildings with and without the presence of active vibration control systems caused by the earthquake hazard scenario using the probabilistic framework (Figure 1). In this regard, a Monte-Carlo simulation method with the 6000 samples is launched. For generating each realization of this simulation, the major building properties, including the number of stories of buildings (or building height), stories' stiffness, stories' mass, and stories' yielding forces are modeled as random variables to consider the uncertainties in their construction process. Whereas, from the other side, an earthquake event scenario, containing all probable mainshock-aftershock sequences (MA sequences) during the whole lifetime of building (50 years), as well as their corresponding synthetic stochastic accelerograms are procreated. Then, the building, which has been designed in accordance with the standard design code (BHRC 2014, ASCE 2016), is analyzed under the whole simulated seismic hazard scenario without the presence of any vibration control devices. In the next stage, the structure is re-designed in the presence of active vibration control system using an advanced two-step optimization process. This optimization procedure works on both technical and economic aspects of building characteristics to achieve the best design scheme. After repeating this procedure and providing a required dataset of realization of buildings' responses, the probabilistic loss curves of buildings with and without the presence of active vibration control system under MA sequences are developed to quantify the probability of exceedance of different loss value levels of building.

The outcomes reveal that in the presence of active vibration control system, the loss value of buildings is reduced significantly, especially at more intensive seismic hazard scenarios. The optimal values of decision variables (stories' stiffness, stories' yielding force capacity) of actively controlled buildings are very close to the ones obtained via existing design code procedures for the uncontrolled structures. Besides, it is indicated that by neglecting the effect of aftershocks, as it is common in almost all design codes, the loss value estimation is decreased considerably. Additionally, the active vibration control system shows slightly better performance in reducing the responses and life-cycle costs of taller buildings. Moreover, the effects of seismic input parameters such as peak ground motion acceleration and velocity on the estimated life-cycle costs are evaluated. Generally speaking, the proposed methodology is a capable approach helping the engineers to prove both technical and economical superiority of vibration control devices, as a seismic protective system, to the traditional uncontrolled buildings, in the long term.

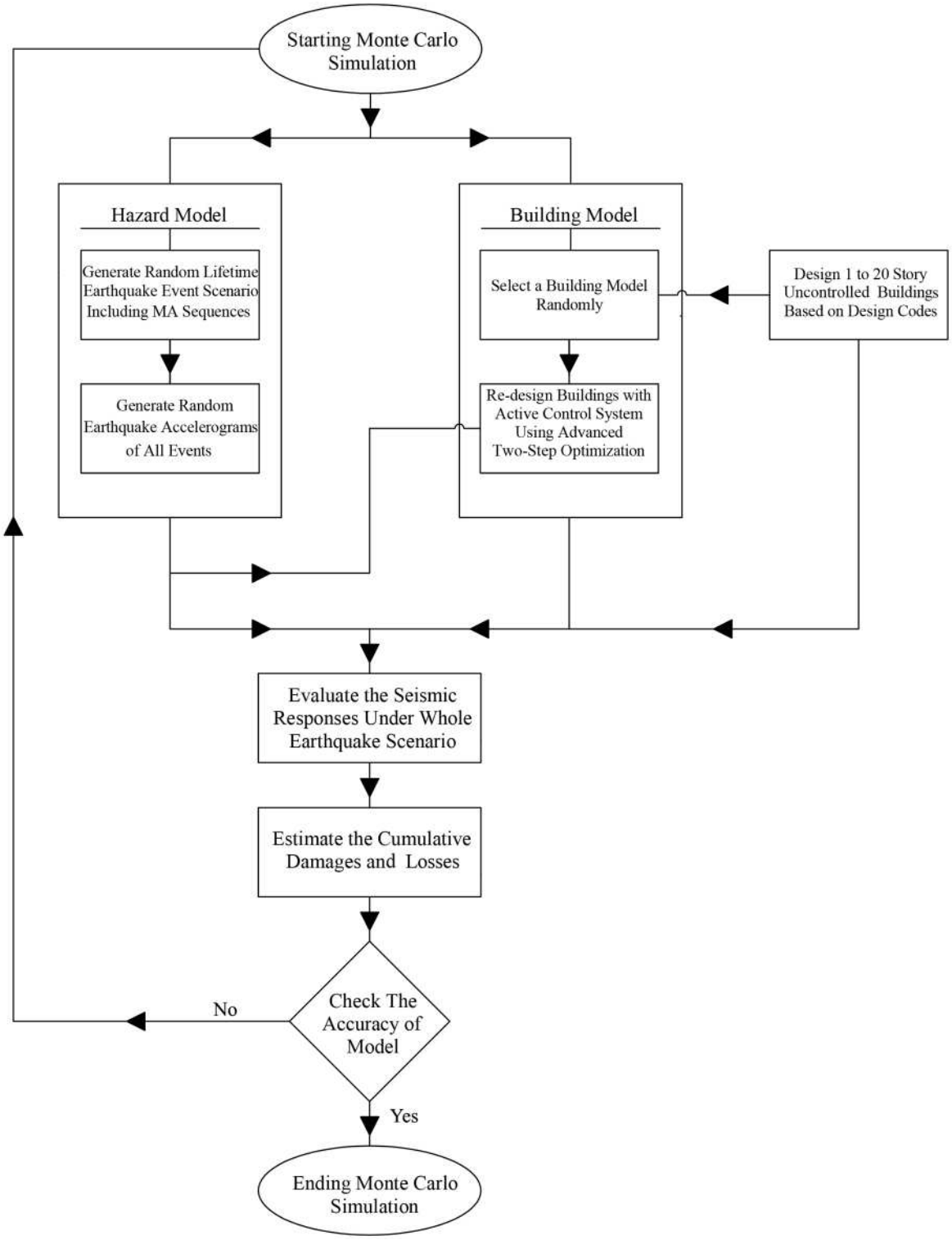


**Figure 1. Flowchart of the proposed lifetime risk assessment of active vibration control system under MA sequences.**

## 2. BUILDING MODELING

In each realization of the Monte-Carlo simulation, it is required to generate a building sample considering the uncertainties in its properties. Here, buildings are modeled as steel shear frame structures, i.e. a one-dimensional nonlinear multi-degree-of-freedom (MDOF) system. In each stick-MDOF model, at least four separate parameters are required to be defined to simulate the building, including the number of degree of freedoms (DOFs), the mass of each DOF, stiffness and yielding force of each nonlinear spring connecting DOFs to each other, and the damping of the system. Accordingly, in this study, the number of building stories, stories' masses,

stories' stiffness, and stories' yielding forces are considered as building model parameters. These parameters reflect both the material and geometry properties of structures. Each of them is prone to different sources of uncertainties. Thus, they are modeled as random variables with defined probability distributions.

In the plan view, it is assumed that each building sample has $15 \times 15$ m dimensions divided into three equal spans in each direction with the dead and live loads equal to 6.5 and 3.0 kN/m$^2$. In the building view, despite the common type of research works, which considers the number of stories of buildings as a deterministic parameter, in this work, it is modeled as a random variable. In other words, it is considered that any building sample for design or analysis can have a different number of stories. In this regard, the statistical data of the constructed residential buildings in the Tehran metro-city during years of 2012 to 2014 are collected (Statistical Center of Iran 2014). The frequency distribution, and consequently probability density function (PDF) of buildings' number-of-stories of this data is extracted for simulating the number of stories of buildings, which are going to be generated in each Monte-Carlo sample. As it is seen in Figure 2, most of the buildings (about 80%), constructed in this time span, are 5, 6, and 7 stories. The total number of buildings with the number of stories equal to or more than 20 is near zero in comparison with the total number of constructed buildings (59 out of 31373). Therefore, only 20 different buildings with the number of stories ranging from 1 to 20 are considered herein.

Next, it is assumed that the other three parameters of building models, i.e. stories' masses, stiffness, and yielding forces, follow the lognormal distribution with the coefficient of variations equal to 0.1, 0.03, 0.07, respectively (Khansefid and Bakhshi 2019a). To obtain the mean values of these variables, first, all of these 20 different buildings' models, on 4 different soil types, are initially designed without the presence of active vibration control system based on the Iranian national seismic code (BHRC 2014) and verified with the international code ASCE7-16 (ASCE 2016). The buildings are presumed to be constructed by the steel material with the yielding stress of 240 MPa. For each building and soil type (according to ASCE7-16 (2016)), all the required properties, including stories' stiffness, and yielding forces are obtained (see appendix A) and considered as mean values of the random variable's PDF.

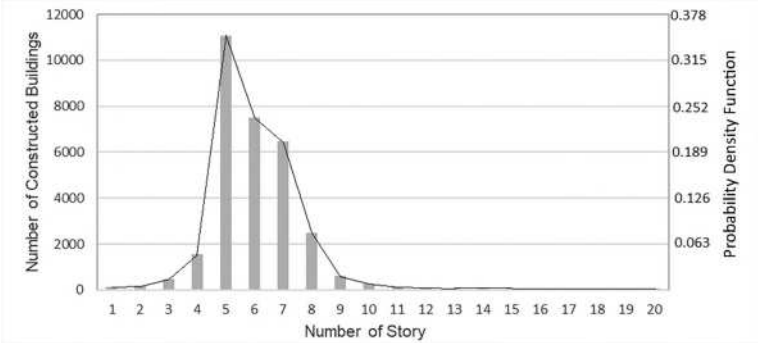


**Figure 2. The number of buildings with the specific number of story in the Tehran metro-city constructed from 2012 to 2014.**

## 3. STRUCTURAL MODEL IN PRESENCE OF ACTIVE VIBRATION CONTROL SYSTEM

The method used for analyzing the structures equipped with the active vibration control system under acceleration time series is a nonlinear stick mass-spring approach to reduce the required analysis runtime. Accordingly, buildings are simulated as a one-dimensional nonlinear MDOF system. The equation of motion of this multi-degree of freedom structure in the presence of an active vibration control system can be written in the below form (Preumont 2011):

$$\mathbf{M}\ddot{\mathbf{x}}(t) + \mathbf{C}\dot{\mathbf{x}}(t) + \mathbf{F_h}(t) + \mathbf{F_a}(t) = -\mathbf{ML}\ddot{x}_g(t) \quad (1)$$

where $\mathbf{M}$, $\mathbf{C}$, $\mathbf{F_h}$, $\mathbf{F}_a$, and $\mathbf{L}$ are mass matrix, inherent damping coefficient matrix, non-linear restoring force vector, active vibration control force vector, and influence vector, respectively. $\ddot{\mathbf{x}}$, $\dot{\mathbf{x}}$, $\mathbf{x}$, and $\ddot{x}_g$ are structural acceleration response vector, relative velocity response vector, relative displacement response vector, and input earthquake acceleration.

The structural nonlinearity of system in equation (1), is simulated by the Bouc-Wen model (Ismail et al. 2009), with the typical shape illustrated in Figure 3**Error! Reference source not found.**. This nonlinear model needs information about three input parameters for each of DOFs to be applicable, including initial stiffness ($k$), yielding force ($F_y$), and the ratio of secondary to initial stiffness ($\alpha$) of the system. The first two parameters were obtained previously for each model at each story. The latter is obtained for all buildings on all soil types by performing the push-over analysis (see appendix A). Moreover, the structural inherent damping ratio is

calculated via the Rayleigh method (Chopra 2011) with an assumed 5% damping ratio for the first and third natural vibration modes.

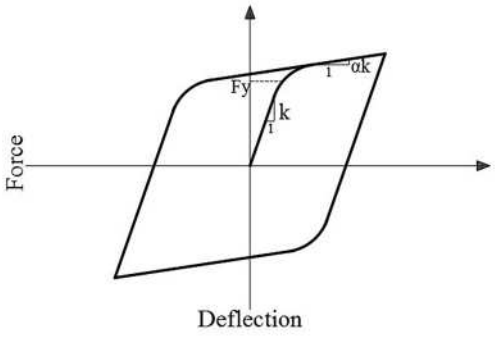


**Figure 3. The typical shape of non-linear Bouc-Wen model force-displacement relationship.**

The well-known and widely used active vibration control algorithm called the linear quadratic regulator (LQR) algorithm is adopted in this research due to its simplicity, accuracy and low required solving runtime. This algorithm first was developed for the linear structures (Soong 1990), However, later its capability to improve the response of nonlinear steel structures is proved (Khansefid and Ahmadizadeh 2016). The amount generated force by the active control system can be obtained via the following equation:

$$\mathbf{F_a}(t) = \mathbf{D}\mathbf{U}(t) \tag{2}$$

where **D** and **U** are the active vibration control device location matrix and control force vector. The latter is obtained by minimizing the LQR objective function, **J**, in the state space as follows:

$$\mathbf{J} = \int_0^t [\mathbf{Z}^{\mathrm{T}}(t)\mathbf{Q}\mathbf{Z}(t) + \mathbf{U}^{\mathrm{T}}(t)\mathbf{R}\mathbf{U}(t)]dt \tag{3}$$

where **Z** is the combined vector of displacement and velocity. **Q** and **R** are weighting matrices of displacement and control force, respectively. The weighting matrices are selected as suggested by Khansefid and Ahmadizadeh (2016) in the following form:

$$\mathbf{Z}(t) = \begin{Bmatrix} \mathbf{x}(t) \\ \dot{\mathbf{x}}(t) \end{Bmatrix} \tag{4}$$

$$\mathbf{R} = \mathbf{I}_{n\times n} \tag{5}$$

$$\mathbf{Q} = 10^{\beta}\mathbf{I}_{n\times n} \tag{6}$$

where **I** is the identity matrix, $n$ is equal to two times of the total number of structural degrees of freedom, and $\beta$ is a coefficient that should be determined for each design via the tuning procedure, i.e. the optimization for each structural property and external loading.

To model building responses more realistically, a force limit is considered for each active vibration control device. In the 1 to 5 story buildings, the 750 KN force limit is considered. For the 6 to 10 story buildings, it increases up to 1500 KN. In the case of 11 to 15 story buildings, it is assumed to be 2250 KN, and for the higher buildings, it is considered to be 3000 KN.

## 4. EARTHQUAKE SCENARIO MODELING

Selection or modeling of the input earthquake excitation for buildings is a very important, and challenging factor that plays a key role in building seismic performance, and risk assessment (Fox and Sullivan 2015, Uribe et al. 2019). In the most of research works and practical design guides (European Committee for Standardization 2004, ASCE 2016), only the average responses of buildings under a set of selected mainshocks are evaluated. However, it was shown by Khansefid et al. (2019a) that, in some cases, the aftershocks can have a considerable intensity, insofar as, their peak ground acceleration (PGA) may reach the mainshock one's or even to the higher levels. Therefore, in this research, it is attempted to model the whole earthquake scenario during the buildings' lifetime, as illustrated in Figure 4, and analyze them under the series of corresponding accelerograms.

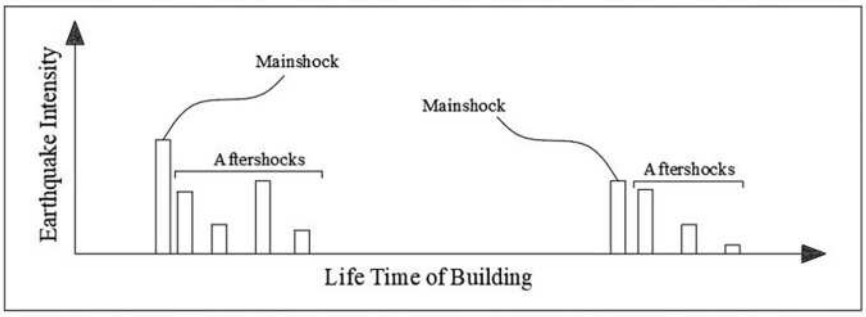


**Figure 4. Schematic of earthquake scenario during the building lifetime.**

The important limitation of buildings performance evaluation under MA sequences during the lifetime of buildings is the lack of appropriate categorized accelerogram database for mainshocks and aftershocks, especially in the case of risk assessment analysis, which needs a large number of analyzes. In order to overcome this problem, herein, the random earthquake scenario model proposed by Khansefid and Bakhshi (2019b) for the Iranian plateau is used. In this regard, a two-step procedure is followed. First, the events scenarios are generated randomly, including the number of mainshocks and aftershocks, as well as their magnitude and occurrence time. Then, in the second step, for each simulated event in the scenario, the corresponding synthetic stochastic accelerogram is procreated.

### 4.1. Simulating Random Earthquake Event Scenario

An earthquake scenario consists of a series of mainshocks and aftershocks. To simulate the whole scenario, it is required to answer the following questions about both mainshocks and aftershocks. How many events will occur? When are their occurrence times? And what are their magnitudes?

For simulating the mainshocks, it is considered that they are independent of each other. This assumption makes it possible to use the Poisson probability distribution (Anagnos and Kiremidjian 1988). Therefore, the number of mainshock events, as well as their seismicity rate, will be obtained by using this PDF in the period of 50 years of building lifetime. Additionally, the time of occurrence of mainshocks will follow the exponential probability density function (Anagnos and Kiremidjian 1988). And finally, the truncated exponential probability density function can simulate the magnitude of each mainshock event according to the following function:

$$P(M)=\frac{B}{1-e^{-B(M_{\max}-M_{\min})}}e^{-B(M-M_{\min})} \tag{7}$$

where $P(M)$ is the yearly probability of occurrence of mainshock with a given magnitude, $M$ is the mainshock magnitude. $M_{min}$, and $M_{max}$ are the lower and upper bound magnitudes assumed equal to 4.0 and 7.7 based on the database of Iranian plateau (Khansefid et al. 2019a). $B$ is an empirical constant that is equal to 2.13 based on the results obtained for Tehran metro-city by Gholipour et al. (2011).

In order to generate the aftershocks' seismological information, the proposed model by Khansefid and Bakhshi (2018) is used. Their model is developed for simulating the properties of aftershocks occurred in the Iranian plateau. Accordingly, the number of occurrence of the aftershocks are obtained by the modified form of Omori formula (Utsa 1969, 1970; Ogata 1988).

$$\lambda(t) = \frac{K_1}{(t + c_1)^{p_1}} \tag{8}$$

where, $K_1$, $p_1$, and $c_1$ are coefficients; and $t$ and $\lambda$ are the time of occurrence and occurrence rate of aftershocks, respectively. These parameters are proposed for the Iranian plateau in the Khansefid and Bakhshi (2018) works. Additionally, for the specific mainshock, with the known magnitude, the occurrence time and the corresponding magnitude of aftershocks are obtained via the empirical joint probability density function presented in their work. As a sample, in Figure 5, the realization of a random earthquake scenario generated for the 50 years is illustrated. The occurrence probability of this 50-year earthquake scenario is 0.00003.

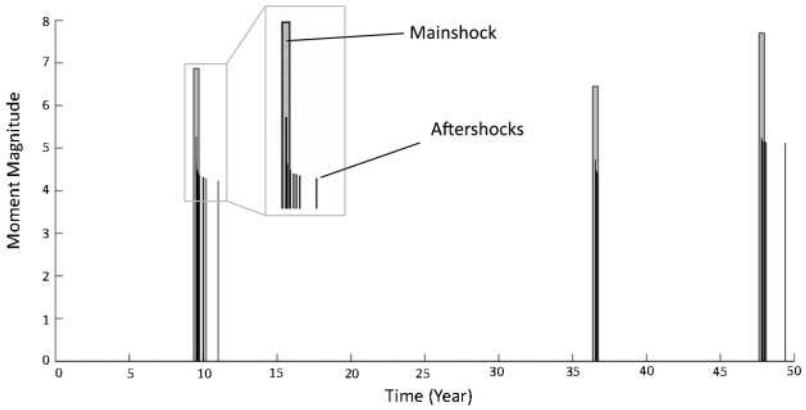


**Figure 5. Sample of generated random event scenario with the probability of 0.00003.**

### 4.2. Simulating Corresponding Accelerograms

The above-mentioned procedure leads to obtain the seismological properties of a random event scenario. Now, for each of the generated events, the corresponding synthetic stochastic accelerogram is procreated through Khansefid et al. (2019b) model capable of considering the mainshock-aftershock categorization as well as pulse-like and non-pulse-like characteristics for the Iranian plateau. This model simulates the earthquake accelerograms by dividing it into two separate parts. The first part is called time modulating function which is responsible for considering the temporal variation of the earthquake records, while the second one, called unit variance process, is used for taking into account the spectral nonstationarity of the signal. This model is applicable for the broad-band signal (far-field) simulation (Rezaeian and Der-Kiureghian 2008, Rezaeian and Der-Kiureghian 2012).

$$X(t) = q(\mathrm{t},\alpha)\left\{\frac{1}{\sigma_f(t)}\int_{-\infty}^{t} h[t-\tau,\lambda(\tau)]w(\tau)\,\mathrm{d}\tau\right\} \tag{9}$$

where X is the earthquake record, $q(t, \alpha)$ is time modulating function, $\left\{\frac{1}{\sigma_f}\int_{-\infty}^{t} h[t-\tau.\lambda(\tau)]w(\tau)d\tau\right\}$ is the unit variance process, $h[t\text{-}\tau, \lambda(\tau)]$ is the unit-impulse response function of the linear filter with the time-varying parameter $\lambda(\tau)$, $\sigma_f(t)$ is the standard deviation of the IRF process, and $w(\tau)$ is the white-noise signal.

The time modulating function is described by:

$$q(\mathrm{t},\alpha) = \begin{cases} 0 & t \le t_{0,q} \\ \alpha_1\left(\dfrac{t-t_0}{t_{\max,q}-t_{0,q}}\right)^{\alpha_2} & t_{0,q} < t \le t_{\max,q} \\ \alpha_1 \mathrm{e}^{-\alpha_3(t-t_{\max,q})} & t_{\max,q} < t \end{cases} \tag{10}$$

where $t_{0,q}$ is the beginning time of the accelerogram, $t_{max,q}$ is the occurrence time of maximum value of the time modulating function, and $\alpha_1$, $\alpha_2$, and $\alpha_3$ are constants.

The unit-impulse response function of the filter frequency can be calculated by:

$$h[t-\tau,\lambda(\tau)] = \begin{cases} \dfrac{\omega_f(\tau)}{\sqrt{1-\zeta_f^2(\tau)}} e^{-\zeta_f(\tau)\omega_f(\tau)(t-\tau)} Sin(\omega_f(\tau)\sqrt{1-\zeta_f^2(\tau)}(t-\tau)) & \tau \le t \\ 0 & otherwise \end{cases} \tag{11}$$

where $\zeta_f$ is the damping ratio of the filter frequency. The frequency of filter ($\omega_f(\tau)$) at any time is expressed by $\omega_0 - (\omega_0 - \omega_n)\frac{\tau}{\tau_0}$ where, $\omega_0$ and $\omega_n$ are the filter frequencies at time $t_{0,q}$, and the end of the time series.

In the case of pulse-like signal simulation, in accordance with the Dabaghi and Der Kiureghian (2017) suggestion, first, a broad-band signal is simulated and then a velocity pulse will be added to the velocity time series of the simulated signal by the following formula:

$$v_{pul}(t) = \left\{\frac{1}{2}V_P \cos\left[2\pi\left(\frac{t - t_{\max,p}}{T_P}\right) + \nu\right] - \frac{D_r}{\gamma T_P}\right\}\left\{1 + \cos\left[\frac{2\pi}{\gamma}\left(\frac{t - t_{\max,p}}{T_P}\right)\right]\right\} \quad (12)$$

$$t_0 - \frac{\gamma}{2}T_P < t \le t_0 + \frac{\gamma}{2}T_P$$

where $T_P$, $V_P$, $t_{max,p}$, $\nu$, and $\gamma$ are pulse duration, pulse amplitude, occurrence time of maximum pulse velocity, phase angle, and oscillatory character, respectively. Moreover, $D_r$ is a variable that eliminates the undesired residual displacement at the end of the pulse, given by:

$$D_r = V_P T_P \frac{\sin(\nu + \gamma\pi) - \sin(\nu - \gamma\pi)}{4\pi(1 - \gamma^2)} \quad (13)$$

The parameters ($\alpha_1$, $\alpha_2$, $\alpha_3$, $\omega_0$, $\omega_n$, $t_0$, $T_P$, $V_P$, $t_{max,p}$, $\nu$, and $\gamma$) of these simulation models are obtained specifically for the Iranian plateau by Khansefid et al. (2019b), applying a linear Bayesian regression approach. In this Bayesian-regression-based model, four input variables, including the epicentral distance, focal depth, average shear wave velocity of 30m underlying soil layer ($V_{s30}$), and the event magnitude, are required to be known for each specific site and earthquake event. The latter is available from the random event scenario generated in the previous step. The other parameters are defined for each event by using their PDFs for the Iranian plateau earthquakes. The best PDFs are acquired by fitting well-known probability density functions, namely, Lognormal, Exponential, Gama, and Weibull, to the data proposed for the Iranian accelerograms database (Khansefid et al. 2019a) by maximizing the negative Log-likelihood method. The results of the most accurate estimators of PDFs are illustrated in Figure 6.

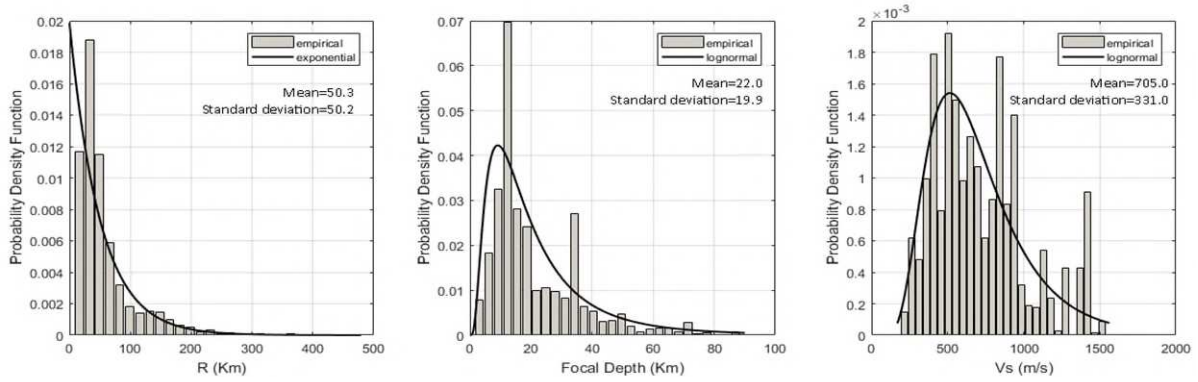


**Figure 6. Probability density functions of the epicentral distance, focal depth, and $V_{s30}$ of recorded accelerograms of Iranian Plateau.**

### 4.3. Statistical Properties of Simulated Scenarios

By using the above-mentioned method, 6000 samples of random earthquake scenarios containing synthetic stochastic accelerograms of mainshocks and aftershocks, compatible with the Iranian plateau condition, are generated as required input variables for the Monte-Carlo simulation procedure. The statistical properties of both seismological information and signal characteristics of all events and accelerograms for all simulated earthquake scenarios are illustrated in Figure 7 considering the differences between mainshock and aftershock events. It is clearly seen that simulated scenarios cover a wide range of events from very low-level intensity to the rare intensive ones. The mainshock magnitudes range between 5.2 to 6.8, and the aftershock ones are between 4 to 5.9. The focal depth (between 0 to 80 km) and source-to-site distance (between 0 to 200 km) are in the rational gamut. The PGAs of signals start from 0.05g and go up to the 0.7g for both mainshocks and aftershocks. Additionally, due to consideration of a wide range of shear wave velocity for the underlying soil layer, simulated signals contain predominant periods ranging from 0.1 to 3 seconds. The strong motion durations (Trifunac and Brady 1975) of mainshocks varying from 3 to 14 seconds, while the aftershock ones are between 2 to 8 seconds. As these random samples are generated using an integrated model considering both seismological properties and earthquake accelerograms simultaneously (Khansefid et al. 2019b), the correlation between different parameters such as duration and PGA, PGA and peak ground velocity (PGV), etc. are taken into account. Thus, it can be stated that the randomly generated earthquake scenarios cover almost all probable ranges of future earthquakes.

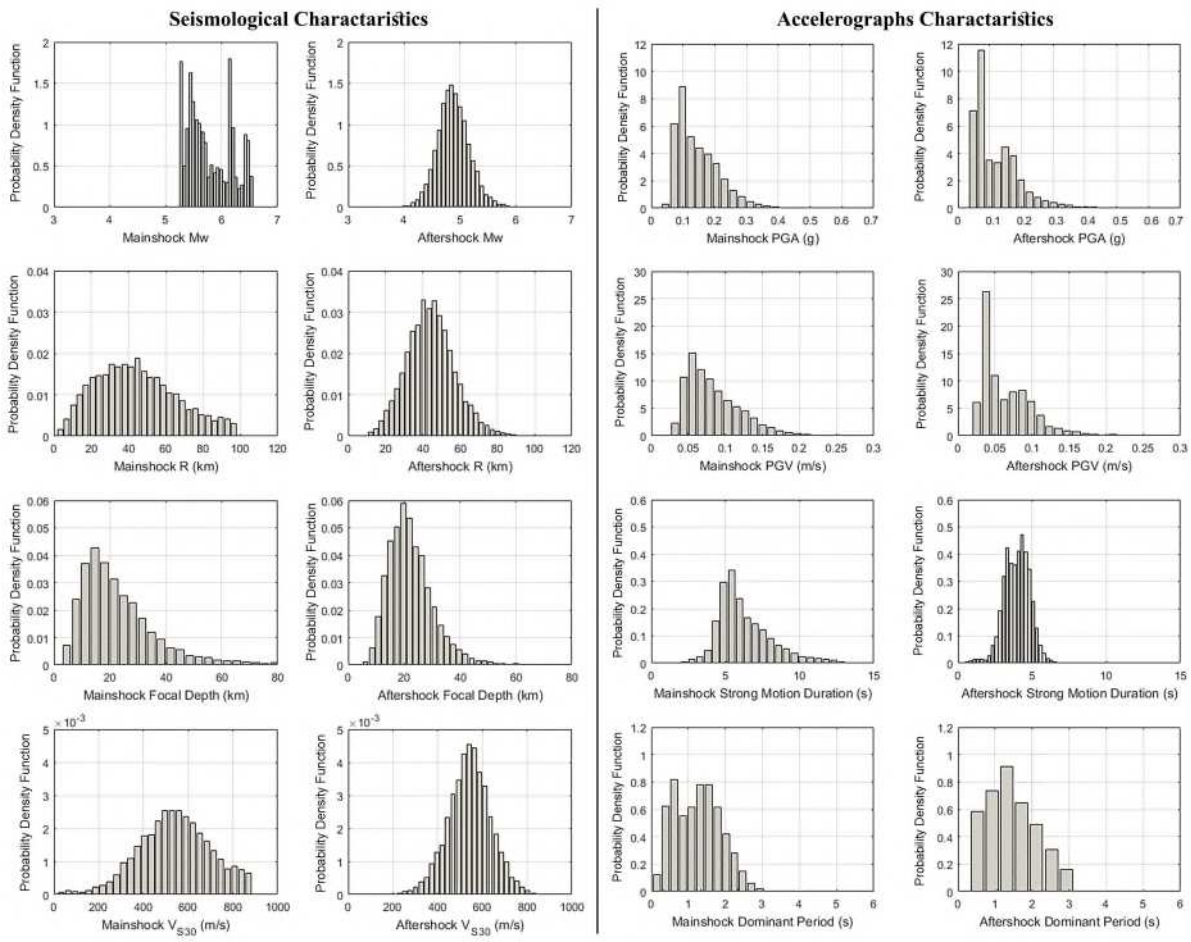


**Figure 7. Seismological properties and Signal characteristics of all simulate earthquake scenario samples.**

## 5. TWO-STEP OPTIMIZATION PROCEDURE

There is no standard design code for designing buildings equipped with the active vibration control system. Additionally, in the literature, there are only limited works that design buildings and vibration control systems concurrently (Khansefid and Bakhshi 2019a, Castaldo and De-Iuliis 2014, Cimellaro 2009). Herein, an advanced two-step optimization process, introduced by Khansefid and Bakhshi (2019a), is used to find the building properties, as well as the active vibration control system parameters simultaneously. Accordingly, for each realization of Monte-Carlo simulation, in the first step, a multi-objective optimization process is performed to minimize both drift and absolute acceleration responses of building concurrently under all accelerograms of the earthquake scenario. In the multiobjective optimization method, instead of obtaining one single optimal solution, a set of results are obtained which are all the candidates of final optimal design. These results are called the Pareto front (Ehrgott 2008). In mathematics, the optimal solutions located on the Pareto front are non-prior, i.e. for selecting one final single optimization result an additional criterion is required. Therefore, in the next stage of our design, among all optimal design samples of the Pareto front, the one which leads to the minimum life-cycle damage cost is selected as a final optimal design. Thereby, this procedure proposes a final design optimized from both technical and economic point of view.

In the optimization process, there are three separate sets of design variables. The first set is the structural stiffness of all stories of a building. The next one is the yielding force at each story, and the last one is the coefficient $\beta$ of the LQR algorithm of active vibration control system. Moreover, in order to achieve feasible optimization results, lower and upper bounds of 0.75 and 1.25 times of the values obtained from the initial design of uncontrolled buildings, based on the existing design codes, are considered as constraints of design variables. For the coefficient $\beta$, the lower and upper bounds are assumed to be 11 and 15 (Khansefid and Bakhshi 2019a).

### 5.1. Multi-Objective Optimization

In order to reduce damages related to different types of structural responses during the earthquake excitation, a multi-objective optimization procedure is applied. Accordingly, two objectives are defined; the average of the

mean of structural inter-story drift under accelerograms of all events of MA sequences, as a first objective (from now on called Drift), and the average of the mean of structural floor absolute acceleration under the accelerograms of all events of MA sequences, as a second objective (from now on called Acc.). It is noteworthy to mention that to model the effect of cumulative damages of buildings under the whole earthquake scenario, the residual drift of buildings at the end of each earthquake excitation is considered as an initial condition at the beginning of the next aftershock.

There are different approaches to solve this multi-objective optimization problem in mathematics (Zitzler et al. 2004), such as aggregated-based, criterion-based, and Pareto front. Among these methods, the latter is selected since it is more generic than the others with fewer limitations. In this research, by using the multi-objective Genetic algorithm (Ehrgott 2008) as a powerful tool, a set of optimal results called Pareto front (Pareto 1927) is obtained. All of these results are non-prior, i.e., none of them can be selected as a final optimal design individually. Therefore, an additional criterion is required.

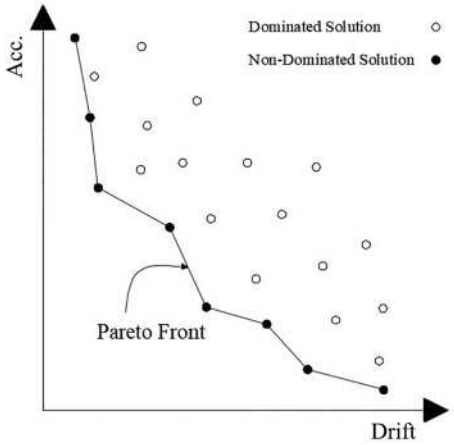


**Figure 8. Schematic of Pareto front in multi-objective optimization.**

### 5.2. Single-Objective Life-Cycle Cost Optimization

In order to distinguish between the samples of the set of non-prior optimal results obtained in the previous optimization step, another optimization process is launched to find a final design sample with the minimum life-cycle damage cost from the Pareto front data.

Herein, different types of damages and losses during the lifetime of buildings due to the earthquake hazard are considered including structural damage cost (STR), non-structural damage cost of drift-sensitive elements (NSD), non-structural damage cost of acceleration-sensitive elements (NSA), building content loss (CON), fatality and injury cost (INJ), and temporary accommodation cost (TAC). To calculate each of these damage costs, among different procedures (FEMA 2001, 2018), the proposed methodology by Hazus (FEMA 2001) is adopted, since it is straight, and developed in accordance with the global response of structures. Accordingly, for any damage type, the probability of facing different damage states (slight, moderate, severe, and complete) is calculated using obtained responses of the building under all events of the earthquake scenario by applying the given fragility curves for steel moment resisting frame building as below:

$$P_i[DS_j \mid RP] = \Phi[\frac{1}{\beta_{DS}} \ln(\frac{RP}{RP_{median}})] \tag{14}$$

where $i$ is the damage type (STR, NSD, NSA, CON, INJ, TAC); $RP$ is the structural response; $RP_{median}$ and $\beta_{DS}$ are the median value and standard deviation of damage state limits (given in Hazus (FEMA 2001) with some minor modifications based on the local condition); $\phi$ is the standard normal cumulative distribution function; and $DS_j$ is the $j^{th}$ damage state.

Afterward, loss values (as a percentage of total value of building and its contents) of each damage type under each earthquake accelerogram are computed by considering all damage levels.

$$\mathrm{E}_i(C) = \sum_{j=1}^{4} P_{i,j} C_{i,j} \tag{15}$$

where $i$ is the damage type, $j$ is the damage state, $\mathrm{E}_i(C)$ is the expected damage cost of each type, as a percentage of building value (construction cost plus its content value), $P_{i,j}$ is the probability of occurrence of damage type $i$ at level $j$ obtained by equation (14), and $C_{i,j}$ is the damage cost of damage type $i$ at level $j$ for residential buildings described in Table 1 (FEMA 2001, Khansefid and Bakhshi 2019a).

**Table 1. Damage state costs of the building as a percentage of building value.**

| Damage Type | Damage cost as a percentage of building | | | |
|---|---|---|---|---|
| | Slight | Moderate | Extensive | Complete |
| Structural | 0.2 | 1.0 | 5.0 | 10.0 |
| Non-Structural, Drift Sensitive | 0.7 | 3.1 | 15.5 | 30.9 |
| Non-Structural, Acceleration Sensitive | 0.6 | 3.1 | 9.5 | 31.8 |
| Contents | 0.2 | 1.2 | 3.6 | 11.9 |
| Temporary Accommodation* | 0.7 | 6.8 | 23.3 | 46.6 |
| Fatality and Injury** | 0.0 | 0.0 | 0.1 | 2.1 |

* The accommodation cost is calculated based on the building recovery time suggested by the Hazus and the rental price of a typical residential building in Iran.
** Fatality and injury cost is calculated based on the probability of occurrence of different injury levels at each damage state based on the Hazus suggestion. In addition, it is assumed that four people live at every 100 square meter area of a building. The ransom cost is considered 85,000$ per person based on the existing Iranian regulations.

At the last step of the optimization process, by summing all damage losses due to all mainshock and aftershock events of each scenario, the total loss value is calculated for any sample of Pareto front optimal designs. Finally, among all samples, the one with the minimum life-cycle damage cost is selected as an optimal design.

## 6. ANALYSIS AND RESULT

To evaluate the life-cycle cost of buildings during their lifetime by considering almost all probable earthquake hazard scenarios, among different types of sampling methods (Mackay 1998, Robert and Casella 2004), such as Monte-Carlo simulation, Importance sampling, Rejection sampling, Metro-police sapling, etc., the first one is adopted as a straight forward method. Accordingly, a large number of input variables is generated randomly, and then the model is run to achieve the results for each sample. This procedure continues to the point that the outputs converge to the final value. In this work, the final goal is to evaluate the total damage cost of steel moment frame buildings without and with optimal active vibration control systems during their lifetime due to the probable earthquake hazard scenarios. There are some important assumptions in the analysis procedure that should be described before dealing with the analysis results.

1) To consider the effects of residual displacement of buildings, it is calculated at the end of each earthquake and applied as an initial condition at the beginning of a next aftershock. In this regard, 30 second zero value acceleration is added to the end of each accelerogram to model buildings' free vibration after each earthquake.
2) In order to evaluate the life-cycle damage costs of buildings more realistically, in any scenario, it is presumed that the damaged building is renovated in three years after the last aftershock.
3) The design procedure (containing both optimization steps) is performed considering all mainshock-aftershock events in each scenario.
4) In the multi-objective optimization process, as it is using the Genetic algorithm for solving the optimization problem (Konak et al. 2006), it is required to set the number of population, and also the number of generations in this algorithm which are selected equal to 100, and 128 respectively (Khansefid and Bakhshi 2019a).
5) All fragility curves and loss values used in this research are for the residential buildings. Additionally, the same fragility curve is used for the damage assessments under both mainshock and aftershock events, which is an acceptable presumption due to low-level damages of structural systems.
6) Buildings' lifetime is considered to be equal to 50 years.
7) It is assumed that the building contents are taken out from the building after the mainshock event by the owner to the safe place.

In this work, a huge number of simulation is performed. 6000 samples are generated in the process of Monte-Carlo sampling. For each sample, to find the optimal design using the two-step optimization method, 6400 models of buildings under the whole accelerogram scenario are analyzed. Therefore, to save the time, only the mainshocks plus its 4 major aftershocks (with the highest PGA) are considered as a whole earthquake scenario, and the weaker aftershocks are neglected. Nevertheless, by this reduction, the total number of building nonlinear time history analysis under all earthquake scenarios reaches to more than 153,000,000. In addition, for the sake of simplicity, all these analyses are done via solving the nonlinear mass-spring stick models of MDOF systems using the Newmark method (Chopra 2011).

In the following parts, after reviewing selected results of building responses with/without the presence of an active vibration control system under one of the randomly generated MA sequences, the loss curve of buildings located in Tehran metro-city for both cases is calculated. Next, the minimum number of required samples for achieving accurate results is investigated. Thereupon, the contribution of different damage types in the total loss

value is assessed. Finally, the sensitivity of obtained life-cycle damage costs to the input parameters is evaluated.

### 6.1. Structural Responses

As a sample, the results of nonlinear dynamic analysis of the 5-story building with/without the presence of active vibration control system under one of the random earthquake scenarios are presented. The hazard scenario includes a mainshock following by 18 aftershocks. The mainshock magnitude is 5.5, and its aftershocks' magnitudes vary between 3.8 and 4.6. In Figure 9, the acceleration time series of mainshock, accelerogram of the most intensive aftershock, as well as the PGA of events of the whole scenario are shown. The PGA of mainshock event is equal to 0.42g, and it is ranging from 0.04g to 0.10g for the aftershocks. The $V_{S30}$ is 450 m/s, and the site-to-source distance of mainshock event is 40 km, while for the aftershocks, this parameter is fluctuating from 42 to 50 km.

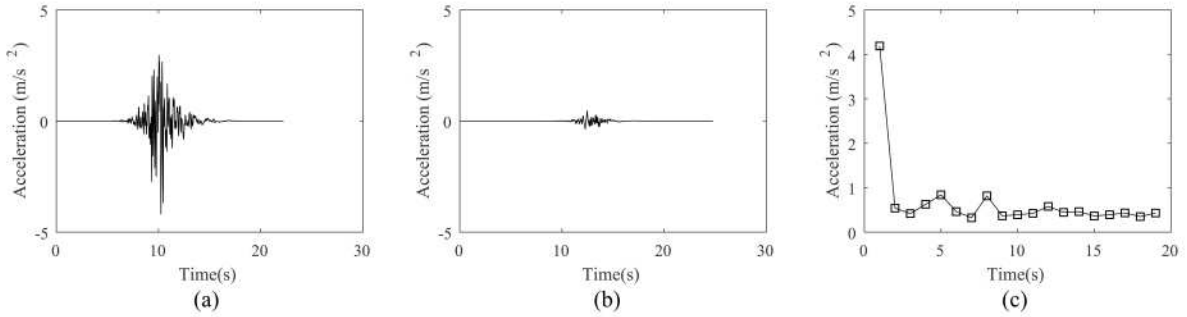


**Figure 9. Properties of selected earthquake scenario. a) Mainshock accelerogram, b) The most intensive aftershock accelerogram, 4th event, c) PGA of all simulated MA events.**

The analysis results, illustrated in Figure 10, prove the superiority of active vibration control system in comparison with the traditional steel moment resisting frame system under MA sequences. It is depicted that the shear-deflection relationship at different stories almost behaves linearly in the presence of active vibration control system (Figures 10-a, 10-b, and 10-c) under the mainshock event. Also, the average of major building responses, including maximum inter-story drift, story absolute acceleration, and story ductility demand under all mainshock-aftershock events decrease significantly at each story, by using the active control system (Figures 10-d, 10-e, and 10-f). Moreover, in Figures 10-g, 10-h, and 10-i, the mean responses of building over all stories are shown for each of the mainshock/aftershock events, which explicitly highlighted the building response improvement by applying the active control system. Interestingly, this system reduces the inter-story drift, story absolute acceleration, and ductility demand of structure about 58%, 62%, and 40%, respectively. In other words, this enhancement is highly salient when noting to this fact that the building almost responds to the earthquakes linearly (ductility demand near 1) while its acceleration response is reduced simultaneously.

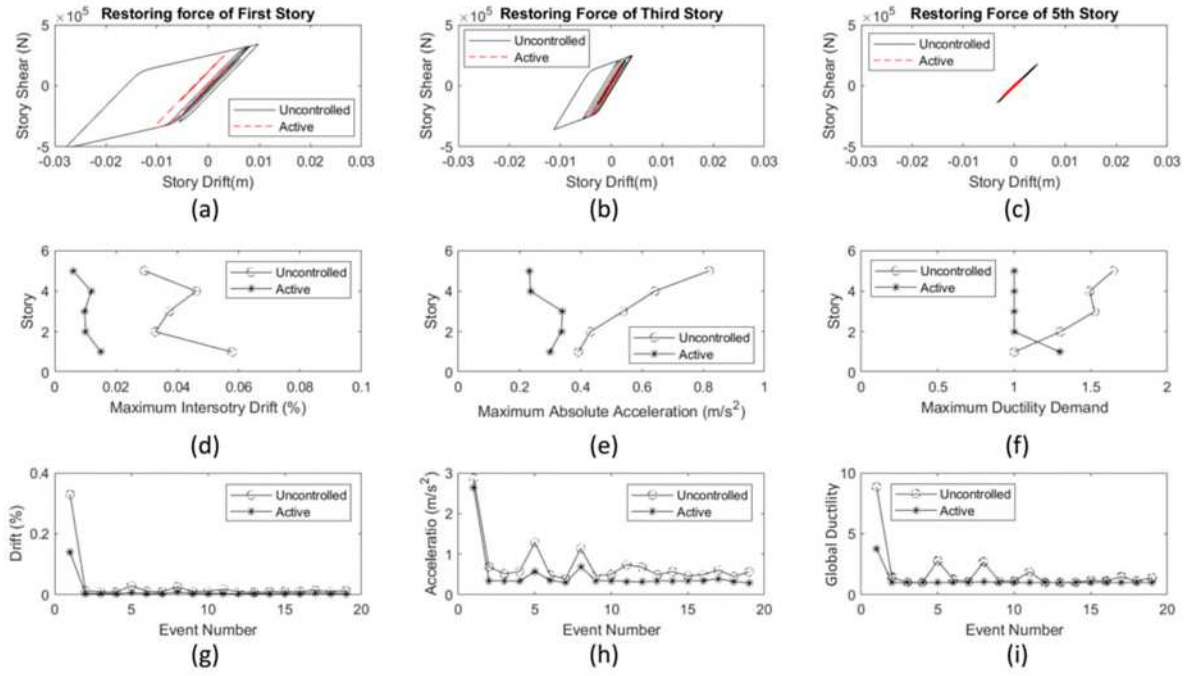

**Figure 10. Structural responses of the 5-story building under one of selected earthquake scenario. a) shear force versus deformation of 1st story under mainshock accelerogram, b) shear force versus deformation of 3rd story under mainshock accelerogram, c) shear force versus deformation of 5th story under mainshock accelerogram, d) average drift response of each story over all events of MA sequence, e) average acceleration response of each story over all events of MA sequence, f) average ductility demand response of each story over all events of MA sequence, g) mean of drift response of all story for all MA events, h) mean of acceleration response of all story for all MA events, i) mean of ductility demand response of the ones of all story for all 19 MA events.**

### 6.2. Loss Curves, Damage Types, and Optimal Design Variables

In this part, an attempt is made to calculate the loss curve of buildings based on their responses to random seismic hazard scenarios in two different cases. The first one is the condition, in which buildings are designed based on the common procedure of existing building design codes, and the other one is the case that all buildings are redesigned via the advanced two-step optimization procedure in the presence of active vibration control systems. By implementing the Monte-Carlo simulation technique the expected loss value can be obtained by:

$$E(C) = \frac{1}{N}\sum_{1}^{N} C_i \tag{16}$$

where $C_i$ is the life-cycle cost of each random sample of the Monte-Carlo simulation, and $N$ is the total number of simulated samples. Here, the value of $N$ is not set from the beginning of simulation process. In other words, during the Monte-Carlo simulation procedure, new samples are generated continuously up to the point that the required accuracy is reached at different loss value levels. Accordingly, 10 equal bins of loss values are defined for the estimated seismic risk of buildings from 0% to 180% of the building value for the uncontrolled structures and 0% to 160% for the actively controlled ones. Then, the simulation process is started and the random samples are generated continuously until the coefficient of variation (COV) of the estimated risk values of samples in all bins drop below 15%. This goal is slightly achieved with a total of 6000 realizations. Figure 11, shows the COV of obtained loss values at different building loss ranges after the ending of simulation process. As it is depicted, for most of the loss bins, the value of COV goes below 15%, except for some limited number of them. These bins are related to cases that are not critical from the decision-maker's point of view, since a very small expected life-cycle damage cost is not important to the building's owner, and, on the other side, an extremely large one is related to a very rare scenario and is somehow out of the attention. As another important point, there are no meaningful differences between the accuracy achieved for the uncontrolled and actively controlled building.

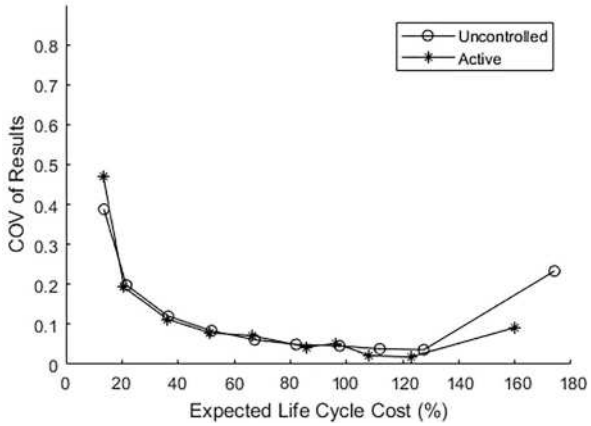


**Figure 11. Coefficient of variation of the expected life-cycle damage cost of buildings in Monte-Carlo simulation.**

By using the database of 6000 random samples, the total loss value of steel moment resisting frame buildings without and with the active vibration control system, located in Tehran metro-city, is obtained and shown in Figure 12. These values are the results of building responses under any probable future earthquake scenario, including mainshocks and aftershocks during structures lifetime (50 years). Additionally, it should be mentioned again that this curve is calculated by considering all common height of the constructed building in Tehran. Therefore, any point of this curve gives the probability of facing a specific damage cost level for any desired steel moment resisting frame building in this city. For instance, the probability level at which a steel structural building located in Tehran metro-city faced a damage cost equal to its initial value (=100%) is 3.5%. If this building was designed with the active vibration control system simultaneously, then the corresponding probability would decrease to 0.1%.

In the structural design codes, always two levels of probability of exceedance of Intensity masseurs (e.g. PGA) are considered as a basis for any seismic hazard evaluation and risk mitigation analysis. The first one is 10% in

50 years (designed base earthquake), and the next one is 2% in 50 years (maximum considered earthquake). Herein, instead of assessing the seismic hazard and risk by the probability of exceedance of ground-motion-related index, a more meaningful measure is proposed. This is the probability of exceedance of facing the life-cycle damage cost of building under any probable future earthquake scenarios in the 50 years life span of the structure. This damage cost is evaluated 53% of building initial value, with the 10% probability of exceedance, and 106% with the 2% probability of exceedance. On the other hand, if the building is equipped with the active vibration control system, damage costs will reduce to 18% and 36% of the initial value of building for 10% and 2% probability of exceedance, respectively. In addition, this diagram prepares a good measure for the stake-holders of buildings to decide whether the application of vibration control system is beneficial for their project or not. For instance, in the probability level of 10% in 50 years, by using the active vibration control system, the life-cycle cost of building will be reduced from 53% to 18% of building value. It means that the building owner can invest in the vibration control system for his/her project up to 35% (=53%-18%) of its final value.

As another important fact, in Figure 12, it is observed clearly that if the effect of aftershocks is not taken into account, then the life-cycle damage cost will be evaluated considerably less than the real condition, e.g., for the 10 and 2 percent probability of exceedance, it is obtained 4.5 % and 8.5% for uncontrolled building. While for the actively controlled structure these values are reduced to 2.7% and 7.7%. On average, by neglecting the aftershocks, the total loss value is evaluated 70% less than the real condition, which is a significant error.

As it was described previously, the number of analysis performed herein is very high. This means that the application of proposed method is highly time-consuming, which may reduce its attractiveness for being used widely by scientists or engineers. Therefore, here, it is examined whether it is possible to estimate the life-cycle cost by the fewer number of samples or not. Accordingly, the sensitivity of obtained loss curves to the number of simulated samples is assessed by Bootstrapping method (Efron and Tibshirani 1993). In accordance with this method, it is assumed that the results calculated from 6000 samples are the real target loss curve of dealing issue. Then, it is hypothetically considered that, instead of 6000 realizations, the total number of generated samples are equal to smaller values, namely 3, 7, 30, and 100. Afterward, for each of them, a set of samples with the total number of members equal to these values are selected from the whole 6000 samples and the loss curve is established for the selected set. This procedure is repeated 10000 times to find the expected loss curve for each defined total number of samples. The results for both uncontrolled and actively controlled buildings are shown in Figure 13. It is indicated that by only generating 3 or 7 samples, the estimated loss curve is tangibly different from the real one. For a total of 30 samples, the accuracy is improved. However, for the extreme scenarios with a high-level loss value, the accuracy is not still sufficient. The set of samples with at least 100 or more members is more or less a good estimator of the target loss curve. Therefore, in general, it may be inferred that, for this risk assessment procedure, it is not needed to generate a large database of analyzed buildings. The minimum number is possible to be set around 100.

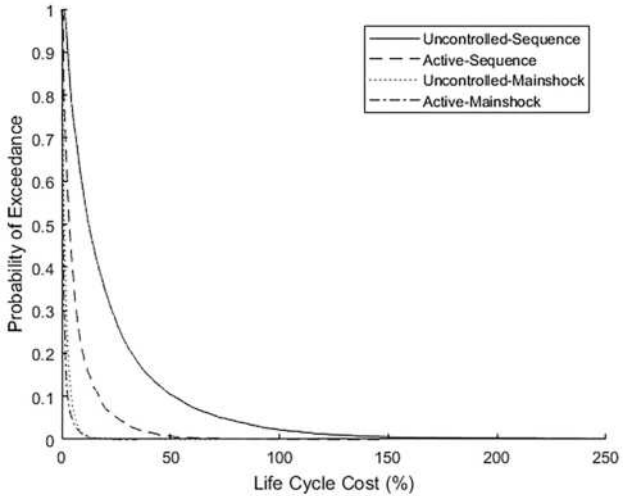


**Figure 12. Loss curve of steel moment resisting frame building without and with active vibration control system, located in Tehran metro-city, under any probable future earthquake scenario.**

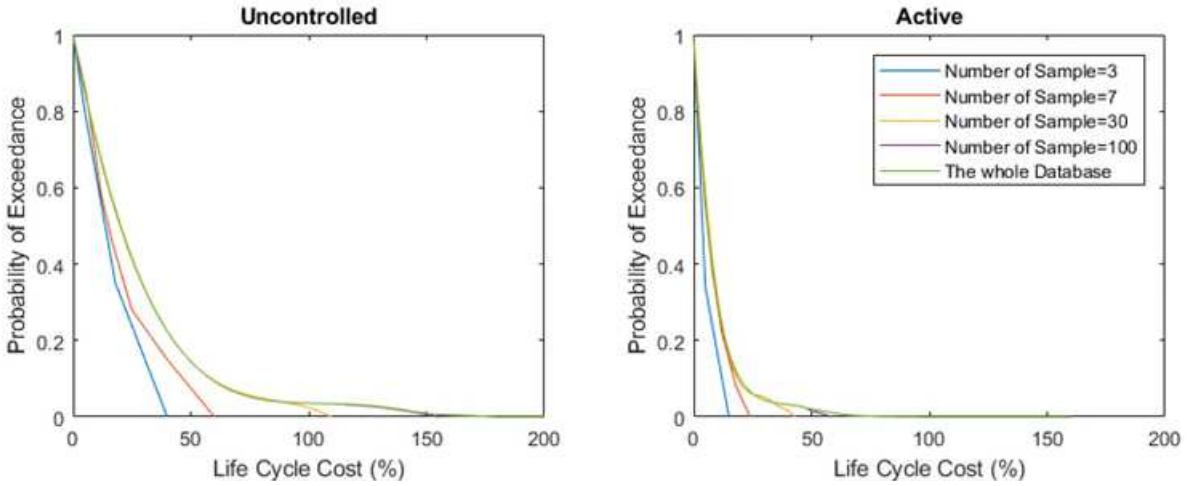


**Figure 13. Results of Bootstrapping method for sensitivity evaluation of sampling method to the number of generated samples.**

The categorization of damage types and identification of their contributions into the total estimated loss value of any building is an important issue that helps to interpret the building behavior correctly. The average contribution of each damage type in the loss curve of buildings without and with the presence of an active vibration control system is illustrated in Figure 14. It is seen that the CON, NSA, NSD, STR, TAC, and INJ damage costs have the highest contribution to the total loss value of buildings, respectively. On average, 72% of building loss value arises from the damage types (CON, and NSA) related to the acceleration response of buildings. This is implicitly pointing out to the fact that the international building codes are successful in their mission to prevent buildings to be damaged by the structural deformation. On the other hand, it is highlighting the necessity of dealing with the control of buildings' acceleration response in future design codes. Moreover, the application of active vibration control system changes the ratio of damage types contributions to the total loss value of building. It causes a reduction in the effect of acceleration-related damage types. As another interesting observation, the loss value related to the fatality and injury is almost near zero which verifies the life-safety performance of buildings designed in accordance with the common international building codes.

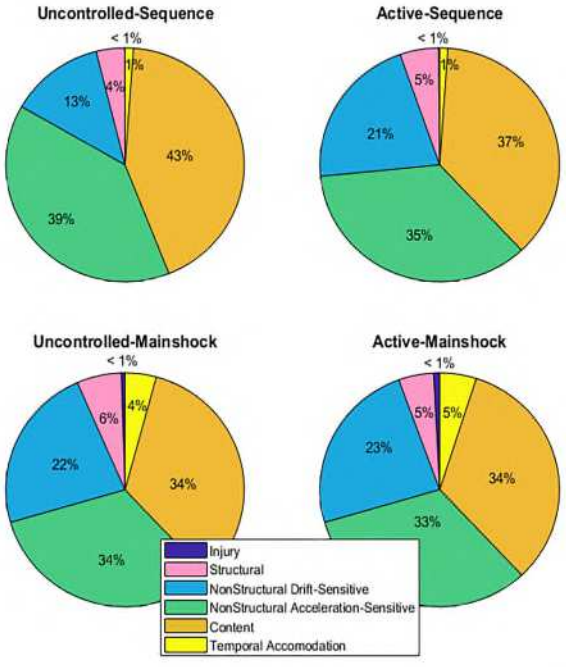


**Figure 14. Contribution of each damage type in the total damage cost of buildings without and with optimally designed active vibration control system during its lifetime in two different cases of considering and neglecting the aftershock events.**

### 6.3. Sensitivity Analysis of Output Results to the Input Parameters

In this part, the sensitivity of analysis results to input variables is investigated, including both building and earthquake scenario properties. The variation of building responses to the height of buildings is one of the most important parameters which always attracts the researchers' attention. In Figure 15, in accordance with the large database of building analysis results, it is indicated that the total life-cycle damage cost of buildings is reduced gradually by the increase in the building height, either it is uncontrolled or equipped with the active vibration control system. Additionally, the standard deviation of results, in the presence of an active vibration control system, shows a significant decrease, which implicitly proves the higher reliability of this system.

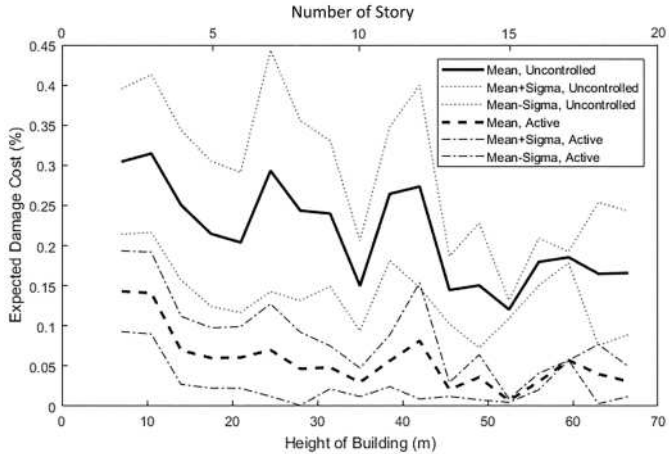


**Figure 15. Variation of the total building life-cycle damage cost to the height of buildings under earthquake scenarios.**

Optimal values of the mean of stories' stiffness, stories' yielding force, and $\beta$ parameter of LQR algorithm for the actively controlled structure, as well as two first parameters for the uncontrolled building, designed based on the common building codes, are illustrated in Figure 16. The results are reported for the mean values, as well as mean plus/minus a standard deviation of results. Generally, the average of building stories' stiffness and yielding forces increase by the increase of the building height. Interestingly, the optimal values of the building properties of actively controlled structures, obtained through the simultaneous optimization process of building properties and active vibration control systems, are slightly (2% on average) smaller than the ones obtained from the building design codes for uncontrolled structures. It means that with acceptable accuracy, instead of an integrated design of building properties and active vibration control system, it is possible to first design a building using the common design codes, then find the optimal active vibration control system properties for the previously designed structure. Moreover, the $\beta$ parameter of LQR algorithm increases with the increase in the building height, i.e. the higher is the building, the more control force is needed.

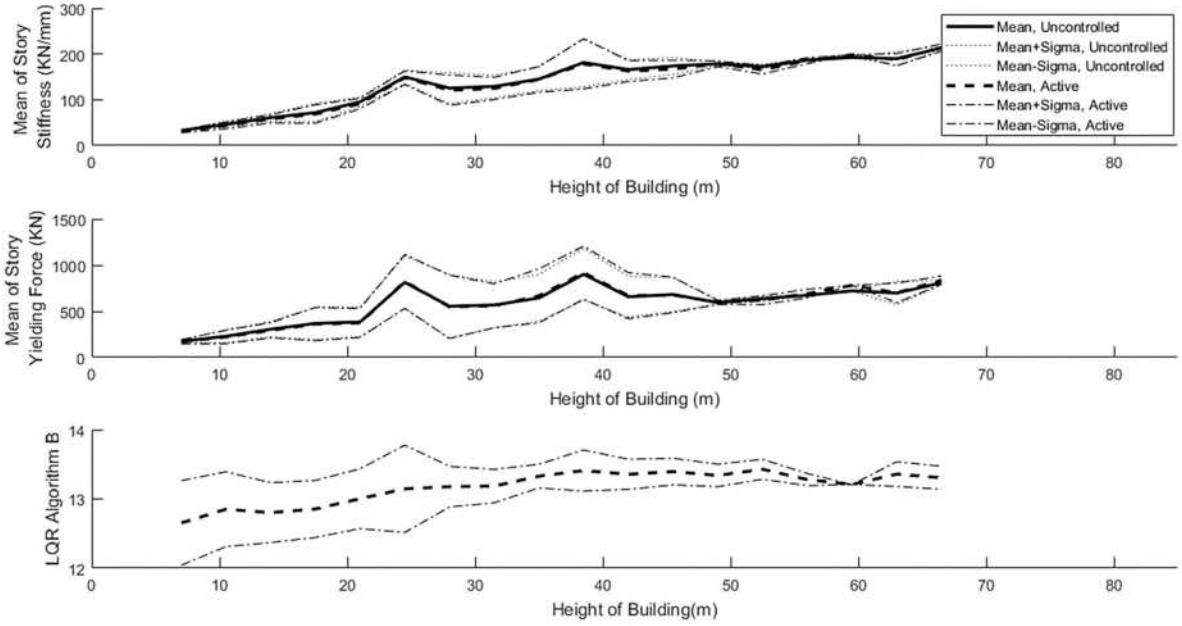


**Figure 16. Variation of building properties (stories stiffness and yielding forces) for both uncontrolled and controlled building as well as optimal $\beta$ parameter of active LQR algorithm due to building height changes.**

The mean value of structural responses under earthquake excitation of all scenarios events with respect to the height of buildings is presented in Figure 17. It is observed that by the increase in the height of building, the structural responses do not change tangibly. However, the drift response is slightly decreased. Equipping the buildings with the active vibration control system causes a significant improvement in all responses; especially, the average of ductility demand of all stories of buildings is decreased from 3.5 for the uncontrolled building to slightly higher than 1.0 in controlled structures. In other words, the active vibration control system is well-capable of improving structural behavior to the point that it vibrates linearly regardless of the building height for low- to mid-rise buildings.

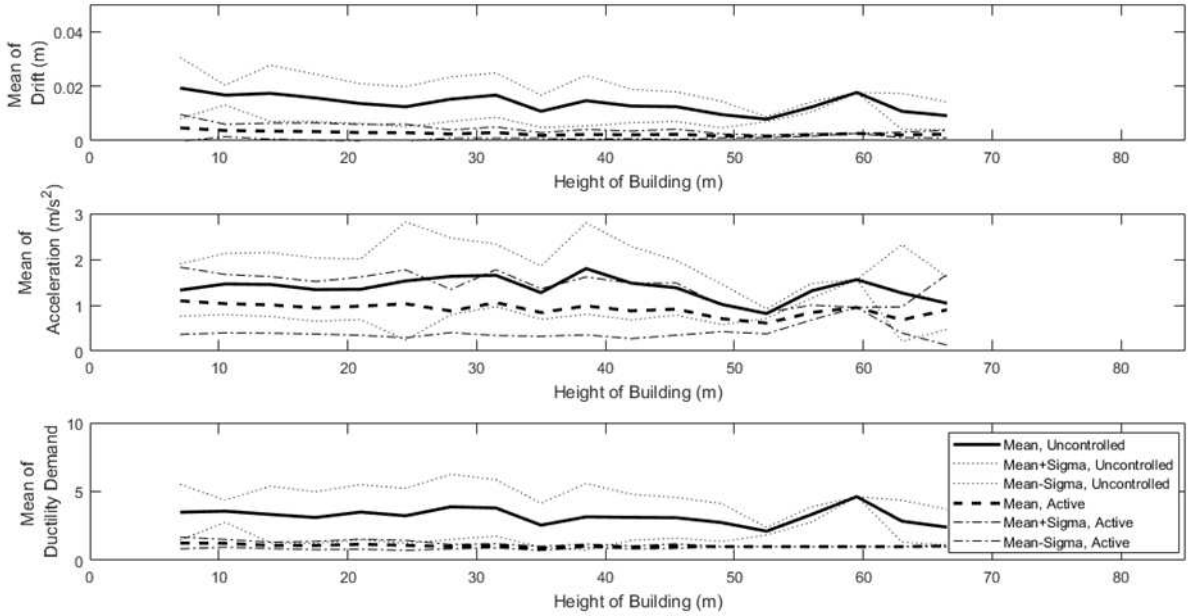


**Figure 17. Variation of the mean value of structural responses of buildings without and with active vibration control system under random earthquake scenarios.**

Life-cycle damage cost is directly influenced by the ground motion movement characteristics. Among the most important features of an earthquake affects buildings behavior, PGA and PGV are considered herein. The dependency of loss values to these parameters are illustrated in Figure 18. These earthquake parameters are the average values throughout the whole earthquake scenario, e.g., the PGA for sequence means that the average of PGA of all events in the scenario, and the PGA for mainshocks means that the average of PGA of all mainshock events in the scenario. For classifying the earthquake scenarios in this figure to the near-field (pulse-like) and far-field (non-pulse-like), the number of near-field events in each scenario is counted. If more than half of the events in each scenario are classified as near-field, then the whole scenario is labeled as near-field. In this figure, it is seen that by the increase in the average PGA value of earthquake scenario, the expected life-cycle cost is increasing fast at the lower value. However, for higher PGAs (0.05g and 0.10g for uncontrolled and controlled structure, and more), the rate of increase is decreased. In addition, the near-field directivity effect is significant in the total damage loss. As expected, the PGVs of near-field scenarios are higher than the far-field ones. This higher PGV leads to more severe damages (20% on average) than far-field scenarios, especially for the higher PGV range. Besides, equipping building to the active vibration control system reduces damage costs tangibly independent of the earthquake type, whether it is pulse-like or non-pulse-like earthquake scenarios.

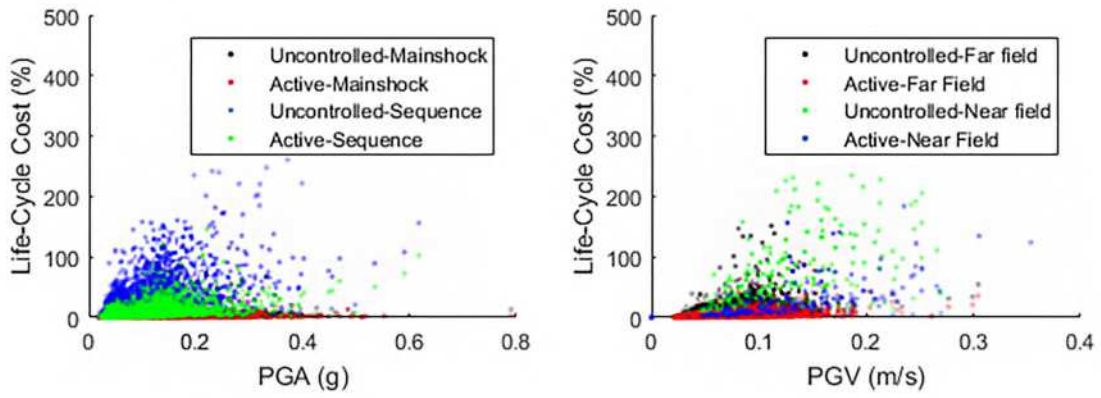


**Figure 18. Life-cycle damage cost sensitivity to the ground motion parameters (PGA, and PGV).**

## 7. CONCLUDING REMARKS

In this research, a probabilistic simulation framework was introduced to evaluate the lifetime seismic risk of non-linear steel moment resisting frame buildings, with/without the active vibration control system (LQR algorithm), under the random probable future earthquake scenario. Building models included 1 to 20 story buildings. Structural properties and active vibration control systems were designed simultaneously as random decision variables with considering their uncertainties. Earthquake scenarios contained almost all probable mainshock and aftershocks with and without forward-directivity velocity pulse effects. Finally, by applying the Monte-Carlo simulation method, a set of 6000 random samples of optimally designed buildings analyzed under the earthquake scenarios which had been produced. The elaborated evaluation of samples' results leads to the remarkable conclusion listed below:

- Equipping a steel moment resisting frame building to the active vibration control system led to a significant reduction in the long-term seismic risk or life-cycle damage cost of building (on average about 66%), especially for the case of more severe scenarios. In addition, this system greatly decreased the average ductility demand of structures from 3.5 to slightly higher than 1.0, which keeps the structures in their linear behavior phase.
- The effect of aftershocks on the evaluation of buildings loss curve was significant, insofar as by neglecting this phenomenon, the final loss value was estimated much less than the real case.
- In this framework, instead of simulating a huge number of randomly generated samples by the Monte-Carlo sampling method, it would be possible to accurately estimate the final loss curve only by assessing 100 random samples of the analyzed building under the earthquake scenarios.
- Among different types of damages considered herein, the ones related to the acceleration response of buildings (CON, and NSA), formed 77% and 67% of total building damages of the uncontrolled and controlled structures, respectively. It highlighted the necessity of dealing with the acceleration-related damage types in future building design codes.
- The optimal properties of actively controlled building (stories' stiffness and yielding forces) were obtained very close to the ones calculated through building design codes for uncontrolled structure. In other words, it is not necessary to design the building and active vibration control system simultaneously, and it can be possible first to design a building based on the codes and standards and then design the active vibration control system for the previously designed structure.
- The near-field scenarios caused about 20% more damages to the buildings during their lifetime in comparison with the far-field scenarios. This is because of the availability of more than 50% pulse-like accelerogram in these generated earthquake scenarios, which contains more input seismic energy.
- The increase in the total height of building from 5m to 67m led to the gradual decrease in the total life-cycle damage cost of buildings. The average structural responses of the building did not change significantly by the increase of building height. However, the drift response slightly was decreased.
- The average of optimal values of stories' stiffness and stories' yielding forces of buildings as well as optimal structural response weighting matrix of active LQR algorithm (coefficient $\beta$) increased with the increase of building height.

Finally, the introduced procedure makes it possible to calculate the seismic risk and loss curve of any desired building during its lifetime for the future probable earthquake scenarios. Therefore, it will be easily possible for decision-makers to prioritize any existing building in a city to whether retrofit it, rehabilitate it, destroy and reconstruct it, or even leave it untouched. In addition, it will make it very convenient to decide whether it would be beneficial to use a vibration control system for a building that is going to be designed and constructed newly or not.

## 8. REFERENCES


American Society of Civil Engineering (ASCE) (2016). *ASCE_07-16: Minimum design loads for buildings and other structures*. Reston, Virginia:

Anagnos T, Kiremidjian AS (1988) A review of earthquake occurrence models for seismic hazard analysis. *Probabilistic Engineering Mechanics* 3(1):3-12.

Becker R (2008) Fundamentals of performance-based building design. *Building Simulation* 1(4):356-371.

Building, Housing and Urban Development Research Center (BHRC) (2014). *Iranian code of practice for seismic resistant design of building*. Tehran: Road, Housing and Urban Development Research Center.

Castaldo P, De-Iuliis M (2014) Optimal integrated seismic design of structural and viscoelastic bracing-damper systems. *Earthquake Engineering & Structural Dynamics* 43(12):1809-1827.

Chopra AK (2011) *Dynamics of Structures-Theory and Applications on Earthquake Engineering*. Prentice Hall: India.

Cimellaro GP, Soong TT, Reinhorn AM (2009) Integrated design of inelastic controlled structural systems. *Structural Control and Health Monitoring* 16(7-8):689-702.

Dabaghi M, Der-Kiureghian A (2017) Stochastic model for simulation of near-fault ground motions. *Earthquake Engineering & Structural Dynamics* 46(6):963-984.

Dang Y., Han, J. P., & Li, Y. T. (2015). Analysis of the seismic performance of isolated buildings according to life-cycle cost. Computational intelligence and neuroscience, 2015.

Dogruel S. (2009) Financial benefits of retrofitting seismic risk building with passive control device. *Improving the Seismic Performance of Existing and Other Structures*, San Francisco, United States.

Ehrgott M (2008) Multiobjective Optimization. *AI Magazine* 29(4):47-57.

European Committee for Standardization (2004) *Eurocode 8: design of structures for earthquake resistance-Part 3: Strengthening and repair of buildings*.

Federal Emergency Management Agency (FEMA) (2001) *HAZUS-MH MR5: Advanced Engineering Building Module*. Washington, DC: Federal Emergrncy Managment Agency (FEMA).

Federal Emergency Management Agency (FEMA) (2018) *Seismic Performance Assessment of Buildings Volume 1 – Methodology Second Edition, FEMA P-58-1*. Washington, DC: Applied Technology Council for the Federal Emergency Management Agency.

Fox MJ, Sullivan TJ (2015) Record-to-record variability in the seismic response of RC walls buildings subjected to ground motions matched to the conditional spectrum. *COMPDYN2015*, Crete, Greece.

Gholipour Y, Y. Bozorgnia, Rahnama M, Berberian M, Ghoreishi M., Talebian, Nazari, Shoja-Taheri J, Shafie A (2011) *Probabilistic seismic hazard analysis- phase 1: greater Tehran Area.* Engineering Optimization Research Group: Tehran.

Gibson EJ (1982) *Working with the performance approach in building*. Rotterdam: CIBdf.

Gidaris I, Taflandis A (2012) Design of Fluid Viscous Dampers for Optimal Lifecycle Cost. *15th World Conference on Earthquake Engineering*, Lisbon, Portugal.

Gidaris I, Taflandis A (2015) Performance assessment and optimization of fluid viscous dampers through life-cycle cost criteria and comparison to alternative design approaches. *Bulletin of Earthquake Engineering* 13:1003–1028.

Hahm D, Ok SY, Park W, Koh HM, Park KS (2013) Cost-effectiveness evaluation of an MR damper system based on a life-cycle cost concept. *KSCE Journal of Civil Engineering* 17(1):145-154.

Ismail M, Ikhouane F, Rodellar J (2009) The Hysteresis Bouc-Wen Model, a Survey. *Archives of Computational Methods in Engineering* 15(2):161-179.

Khansefid A, Ahmadizadeh M (2016) An investigation of the effects of structural nonlinearity on the seismic performance degradation of active and passive control systems used for supplemental energy dissipation. *Journal of Vibration and Control* 22(16):3544-3554.

Khansefid A, Bakhshi A (2018) Statistical evaluation and probabilistic modeling of aftershock sequences of Iranian plateau. *Journal of Seismology* 22(5):1249-1261.

Khansefid A, Bakhshi A (2019a) Advanced two-step integrated optimization of actively controlled nonlinear structure under mainshock–aftershock sequences. *Journal of Vibration and Control* 25(4):748-762.

Khansefid A, Bakhshi A (2019b) New Model for Simulating Random Synthetic Stochastic Earthquake Scenarios. *Journal of Earthquake Engineering*. doi: 10.1080/13632469.2019.1699207.

Khansefid A, Bakhshi A, Ansari A (2019a) Development of Declustered Processed Earthquake Accelerogram Database for the Iranian Plateau: Including Near-Field Record Categorization. *Journal of Seismology* 23(4):869-888.

Khansefid A, Bakhshi A, Ansari A. (2019b) Empirical predictive model for generating synthetic non-stationary stochastic accelerogram of the Iranian plateau: including far- and near-field effects as well as mainshock and aftershock categorization. *Bulletin of Earthquake Engineering* 17:3681–3708.

Konak A, Coit DW, and Smith AE (2006) Multi-objective optimization using genetic algorithms: A tutorial. *Reliability Engineering & System Safety* 91(9): p. 992-1007.

Mitropoulou CC, Lagaros ND, Papadrakakis, M (2011) Life-cycle cost assessment of optimally designed reinforced concrete buildings under seismic actions. *Reliability Engineering & System Safety* 96(10):1311-1331.

Lagaros ND (2007) Life-cycle cost analysis of design practices for RC framed structures. *Bulletin of Earthquake Engineering* 5(3):425-442.

Liu B, Liu M, LI Y (2004) Research and development of performance-based seismic design theory. *13th World Conference on Earthquake Engineering*, Vancouver, Canada.

Loli A, Lamperti Tornaghi M, Negro P (2017) A method to include life-cycle analysis in earthquake design. In Proceedings of the 16th World Conference on Earthquake Engineering-Santiago, Chile.

Mackay DJC (1998) *Introduction to Monte Carlo Methods, in Learning in graphical models*. MIT Press.

Micheli L, Cao L, Gong Y, Cancelli A, Laflamme S, Alipour A (2017) Probabilistic performance-based design for high performance control systems. *Proceeding of Smart Structures and Materials and Integrated System*, Portland, United States.

Mitropoulou CC, Lagaros ND (2016). Life-cycle cost model and design optimization of base-isolated building structures. *Frontiers in Built Environment* 2:27.

Noureldin M, Kim J (2021) Parameterized seismic life-cycle cost evaluation method for building structures. Structure and Infrastructure Engineering 17(3):425-439.

Ogata Y (1988) Statistical Models for Earthquake Occurrences and Residual Analysis for Point Processes. *Journal of the American Statistical Association* 83(401):9-27.

Pareto V (1927) *Manuel d'economie Politique*. Paris: Giard.

Park KS, Koh HK, Hahm D (2004) Integrated optimum design of viscoelastically damped structural systems. *Engineering Structures* 26(5):581-591.

Park G, Micheli L, Cao L, Gong Y, Cancelli A, Laflamme S (2017) Probabilistic performance-based design for high performance control systems. *SPIE Smart Structures and Materials + Nondestructive Evaluation and Health Monitoring*. Portland, United States.

Preumont A (2011) *Vibration control of active structures.* Springer.

Rezaeian S, Der-Kiureghian A (2008) A stochastic ground motion model with separable temporal and spectral nonstationarities. *Earthquake Engineering & Structural Dynamics* 37(13):1565-1584.

Rezaeian S, Der-Kiureghian A (2012) Simulation of orthogonal horizontal ground motion components for specified earthquake and site characteristics. *Earthquake Engineering and Structural Dynamics* 41(2):335-353.

Robert CP, Casella G (2004) *Monte Carlo Statistical Methods. 2nd Edition*. Springer.

Rabonza ML, Lallemant D (2019) Accounting for Time and State-Dependent Vulnerability of Structural Systems. *13th International Conference on Applications of Statistics and Probability in Civil Engineering*, Seoul, South Korea.

Ruiz R, Taflanidis A, Lopez-Garcia D, and Vetter CR (2016) Life-cycle based design of mass dampers for the Chilean region and its application for the evaluation of the effectiveness of tuned liquid dampers with floating roof. *Bulletin of Earthquake Engineering* 14:943–970.

Scozzesea F, Dall'Astaa A, Tubaldib E (2019) Seismic risk sensitivity of structures equipped with anti-seismic devices with uncertain properties. *Structural Safety* 77:30-47.

Shia F, Saygilib G, Ozbulutc O, Zhoua Y (2020) Risk-based mainshock-aftershock performance assessment of SMA braced steel frames. *Engineering Structures* 212:110506.

Soong TT (1990) Active Structural Control: Theory and Practice. Longman Scientific and Technical.

Statistical Center of Iran (2014) *Number of Issued Construction Permission for Buildings of Tehran*, Tehran, Iran.

Trifunac MD, and Brady AG (1975) A study on the duration of strong earthquake ground motion, *Bulletin of the Seismological Society of America* 65:581-626.

Uribe R, Sattar S (2019) Speicher MS, Ibarra L. Effect of Common U.S. Ground Motion Selection Methods on the Structural Response of Steel Moment Frame Buildings Show less. *Earthquake Spectra* 35(4): 1611-1635.

Utsa T (1970) Aftershocks and earthquake statistics (II) further investigation of aftershocks and other earthquake sequences based on a new classification of earthquake sequence. *Journal of the Faculty of Science, Hokkaido University, Series VII* 3:197-266.

Utsa T (1969) Aftershocks and earthquake statistics (I)-some parameters which characterizes an aftershock sequence and their interrelation. *Journal of the Faculty of Science, Hokkaido University, Series VII* 3:129-195.

Vitiello U, Salzano A, Asprone D, Di Ludovico M, Prota A (2016) Life-cycle assessment of seismic retrofit strategies applied to existing building structures. *Sustainability* 8(12):1275.

Wen YK, Shinozuka M (1997) Cost-effectiveness in active structural control. *Engineering Structures* 20(3): 216:230.

Yamawaki K, Kitamura H, Tsuneki Y, Mori N, Fukai S (2000) Introduction of a performance-based design. *12th World Conference on Earthquake Engineering*, Auckland, New Zealand.

Zitzler E, Laumanns M, Bleuler S (2004) *A Tutorial on Evolutionary Multiobjective Optimization, in Metaheuristics for Multiobjective Optimisation*. Springer 3-37.

## APPENDIX A

Here, the complete results of buildings design (stories' stiffness, stories' yielding force, and Bouc-Wen $\alpha$ parameter) described in sections 2 and 3 are presented elaborately.

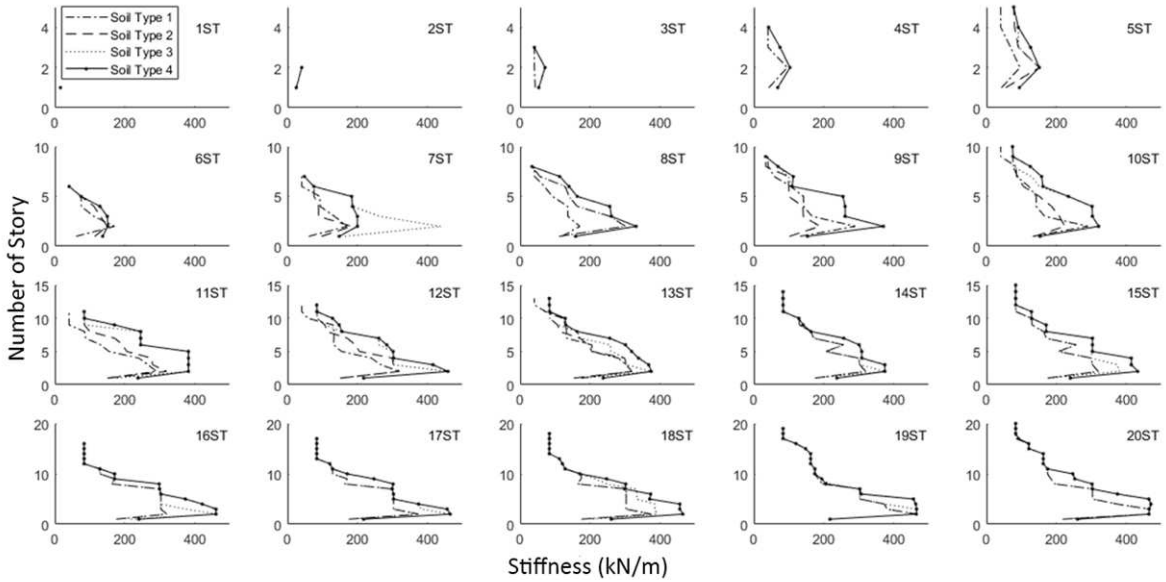


**Figure A.1. Stiffness of each story of all the building models for all different soil types.**

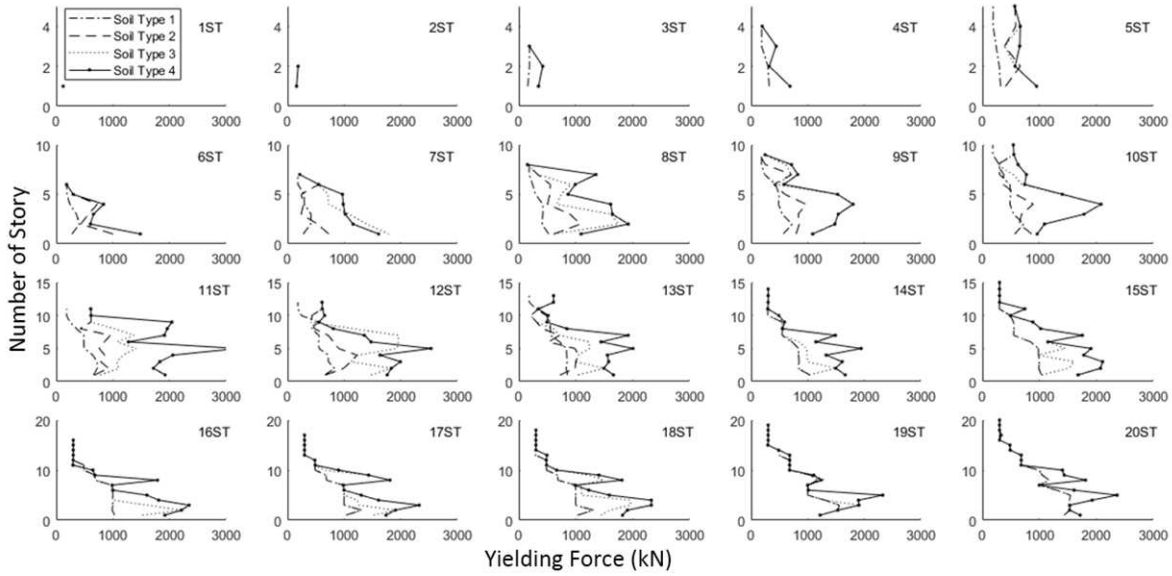


**Figure A.2. Yielding force of each story of all the building models for all different soil types.**

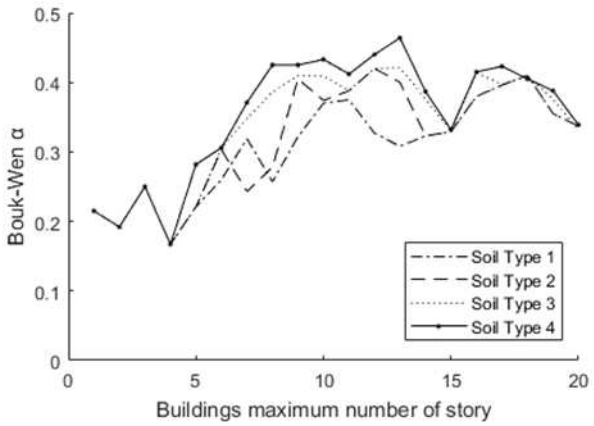


**Figure A.3. Bouc-Wen α parameter of each building model for all different soil types.**

**APPENDIX B**

This appendix presents a glossary of important terms in this paper.

**Table B.1. Glossary.**

| Term | Definition |
|---|---|
| Accelerogram | The recording of ground acceleration as a function of time during a seismic event. |
| Active Vibration Control System | A system that mitigate the building undesired vibration due to input noises (earthquake excitation) via an online procedure using an external power source. |
| Broad-band Signal | Earthquake signals which covers a wide range of frequency and here is used as a representative of far-field earthquakes. |
| Content Damage | All damages occurred to the equipments, staffs, and indoor appliance existed in the building due to earthquake. |
| Cumulative Damage | Damages caused by sequential earthquakes which are added to the damages from the previous event. |
| Earthquake Scenario | A scenario which includes probable mainshocks and aftershocks in a specific time range. |
| Fragility Curve | A curve which shows the probability of facing different levels of damages in a building based on the hazard intensity or building responses to that hazard. |
| Life-cycle Cost | The estimated probable damage cost of building due to life time seismic hazard. |
| Lifetime | 50 years as a period of buildings life span. |
| Loss Curve | The curve showing the probability of exceedance of different ranges of building losses due to seismic hazard. |
| MA Sequence | Sequences of the mainshock and aftershock. |
| MDOF | Multi degree of freedom systems. |
| Multi-Objective Optimization | A method of optimizing a problem with more than one optimization target. |
| Pareto Front | All the optimal results of a multi-objective optimization problem in the method of Pareto. |
| Pulse-like Signal | An earthquake record which its velocity time series contains a pulse due to forward directivity phenomenon. |
| Realization | Generated sample of a random variable. |
| Seismic Risk | The estimated probable loss of buildings due to the future earthquakes. |
| Story Stiffness | The resistance of each building story against a unit deformation. |
| Story Yielding Force | The force level that causes a story of building enters its nonlinear behavior phase. |

# Figures

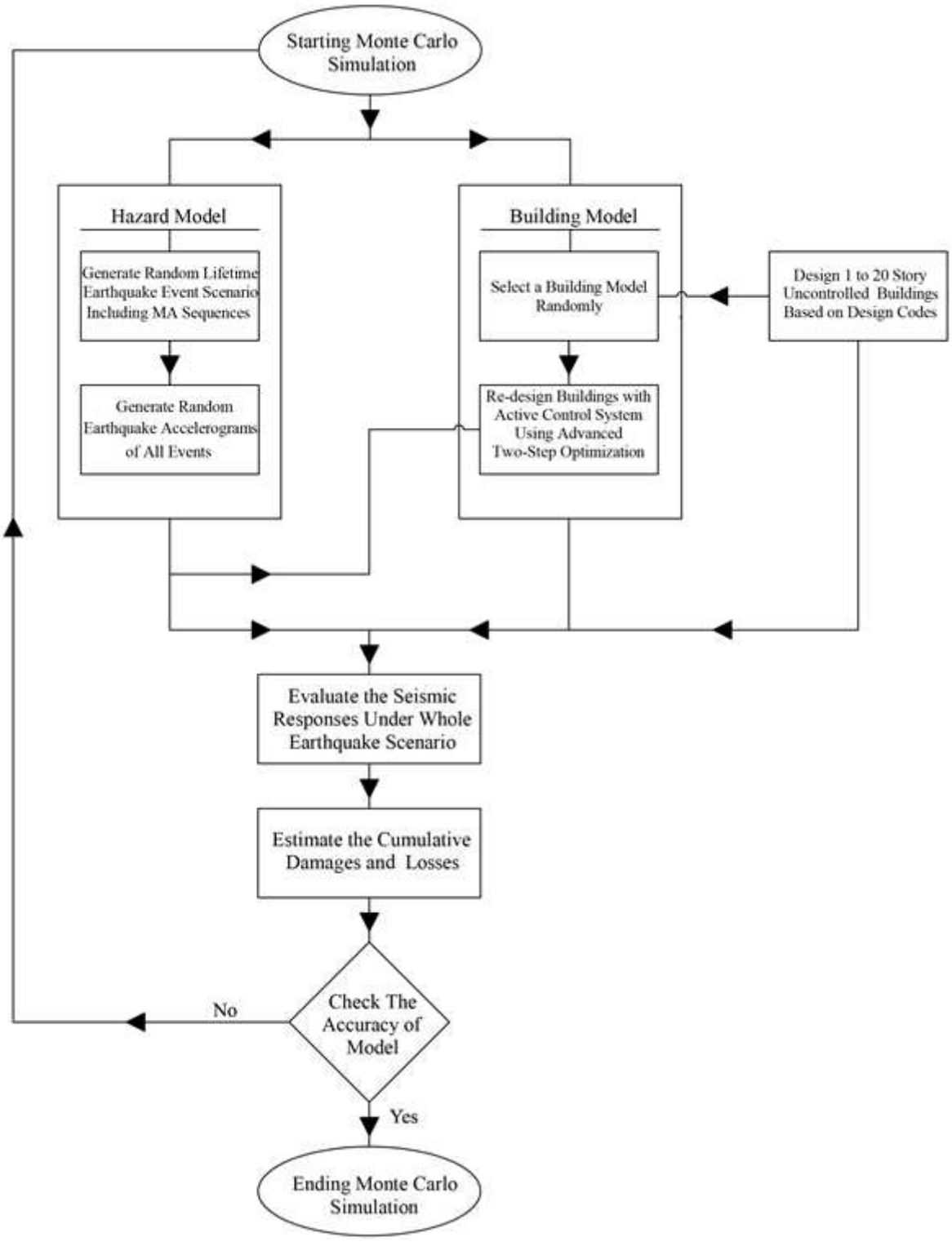


**Figure 1**

Flowchart of the proposed lifetime risk assessment of active vibration control system under MA sequences.

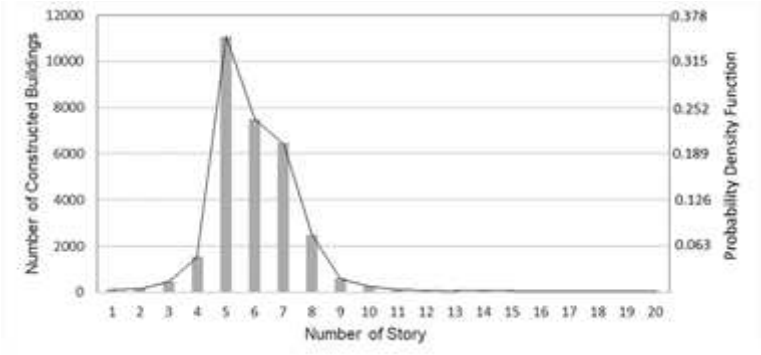


**Figure 2**

The number of buildings with the specific number of story in the Tehran metro-city constructed from 2012 to 2014.

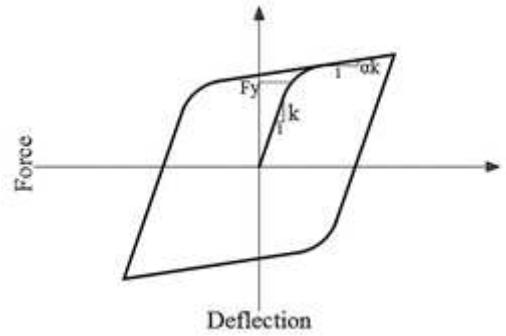


**Figure 3**

The typical shape of non-linear Bouc-Wen model force-displacement relationship.

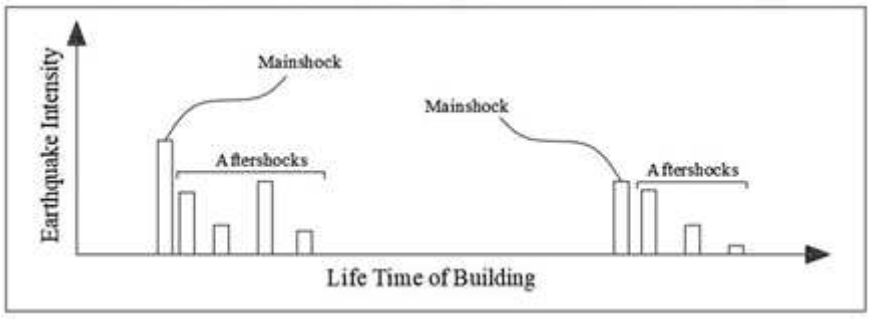


**Figure 4**

Schematic of earthquake scenario during the building lifetime.

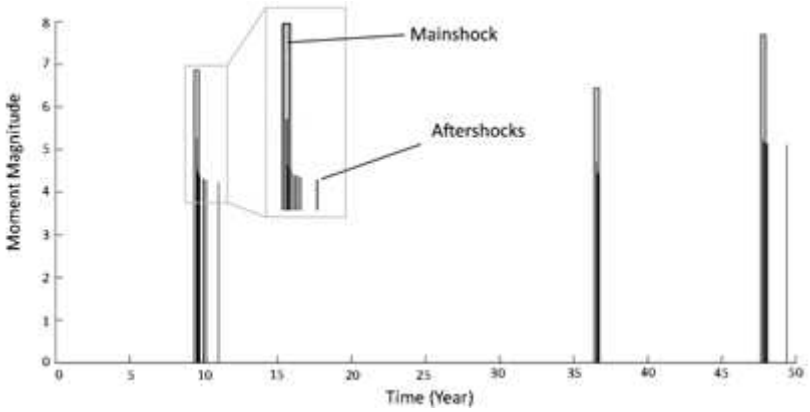


## Figure 5

Sample of generated random event scenario with the probability of 0.00003.

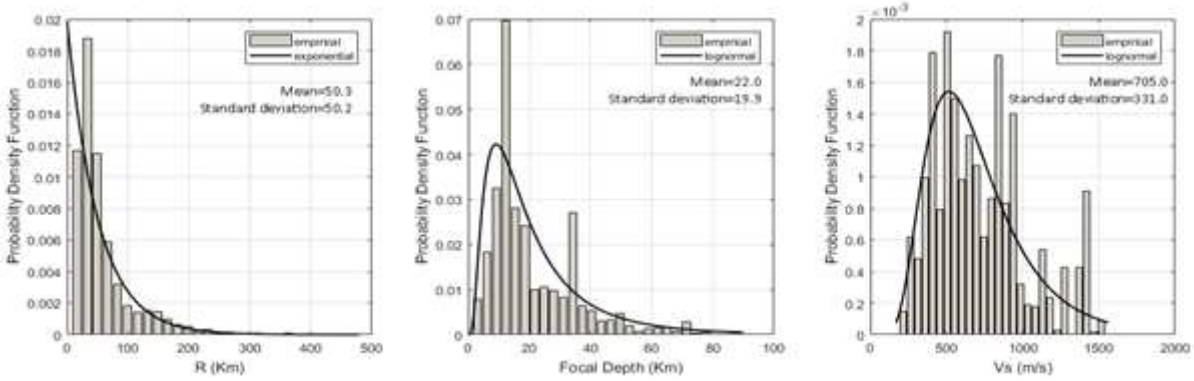


## Figure 6

Probability density functions of the epicentral distance, focal depth, and Vs30 of recorded accelerograms of Iranian Plateau.

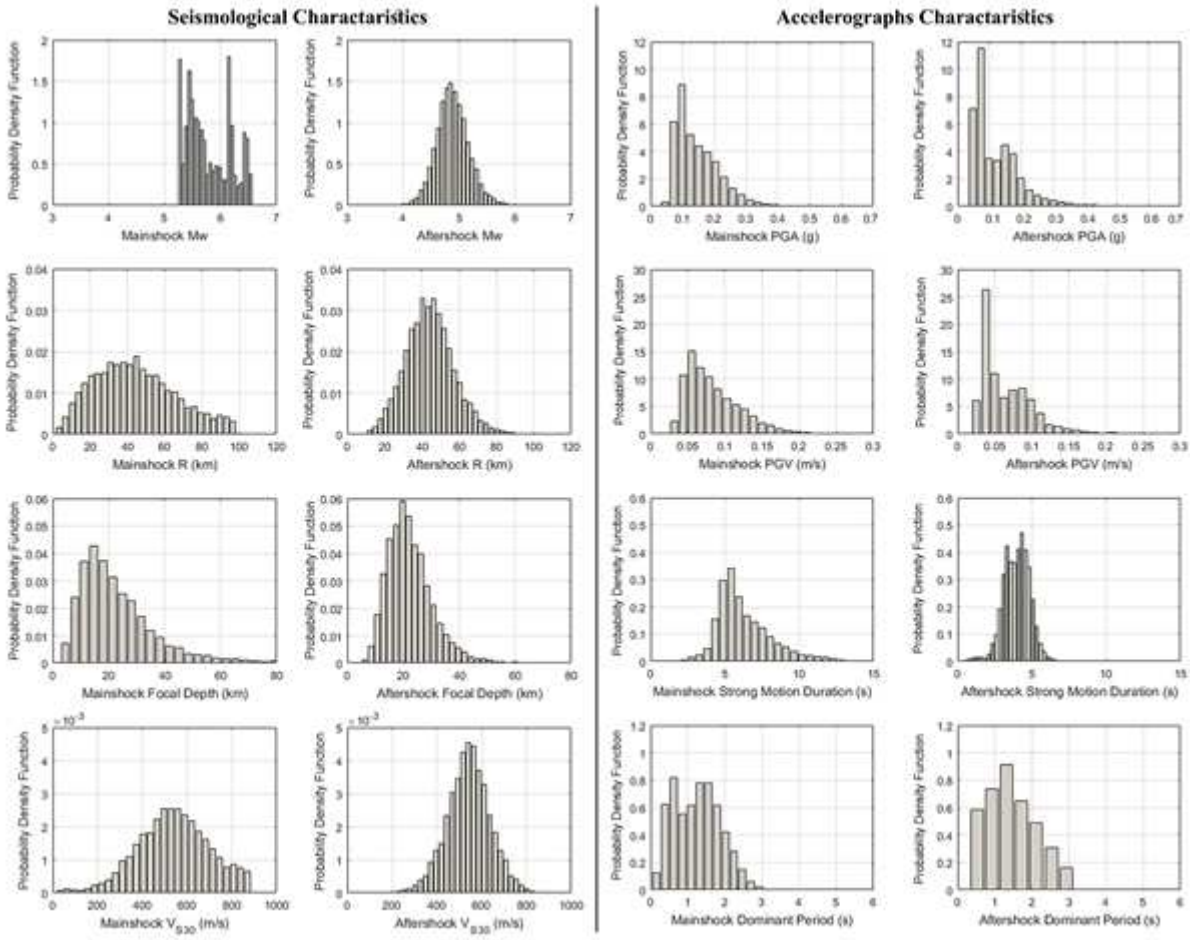


## Figure 7

Seismological properties and Signal characteristics of all simulate earthquake scenario samples.

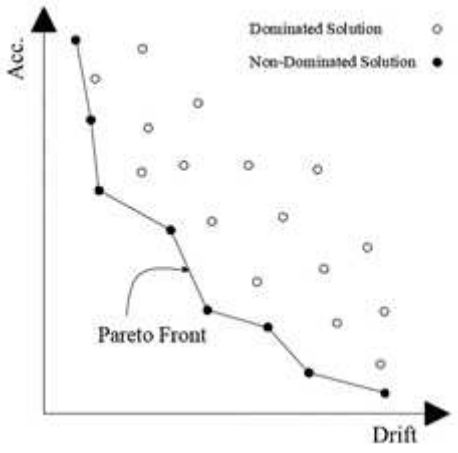


## Figure 8

Schematic of Pareto front in multi-objective optimization.

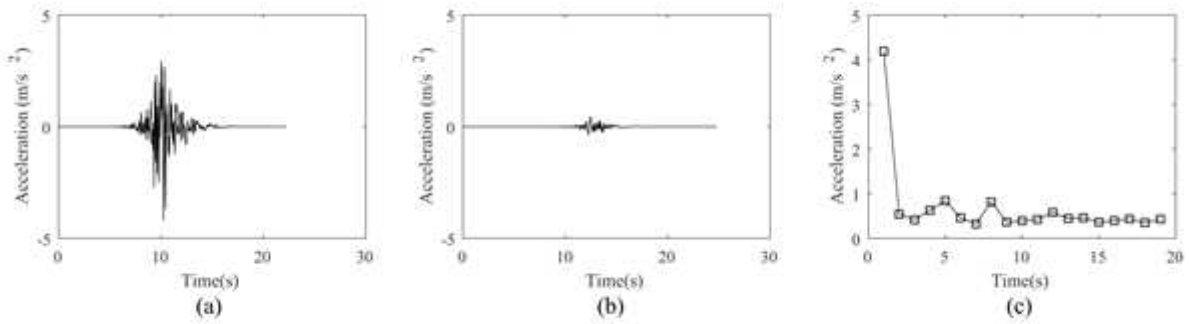


**Figure 9**

Properties of selected earthquake scenario. a) Mainshock accelerogram, b) The most intensive aftershock accelerogram, 4th event, c) PGA of all simulated MA events.

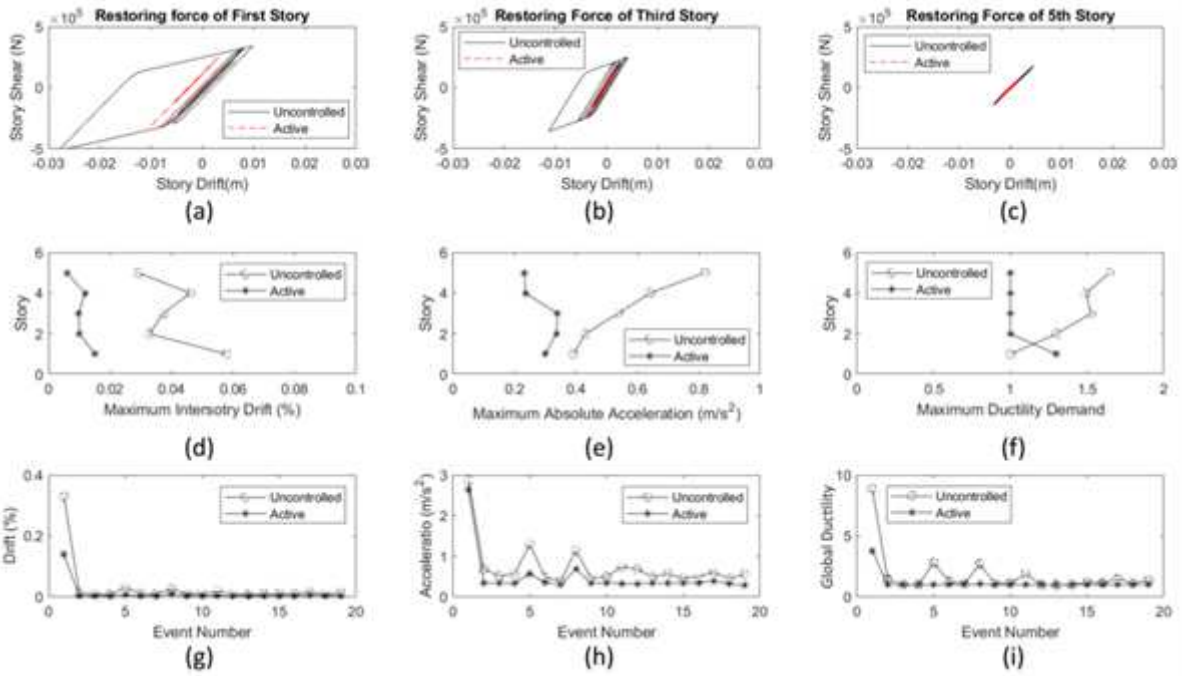


**Figure 10**

Structural responses of the 5-story building under one of selected earthquake scenario. a) shear force versus deformation of 1st story under mainshock accelerogram, b) shear force versus deformation of 3rd story under mainshock accelerogram, c) shear force versus deformation of 5th story under mainshock accelerogram, d) average drift response of each story over all events of MA sequence, e) average acceleration response of each story over all events of MA sequence, f) average ductility demand response of each story over all events of MA sequence, g) mean of drift response of all story for all MA events, h) mean of acceleration response of all story for all MA events, i) mean of ductility demand response of the ones of all story for all 19 MA events.

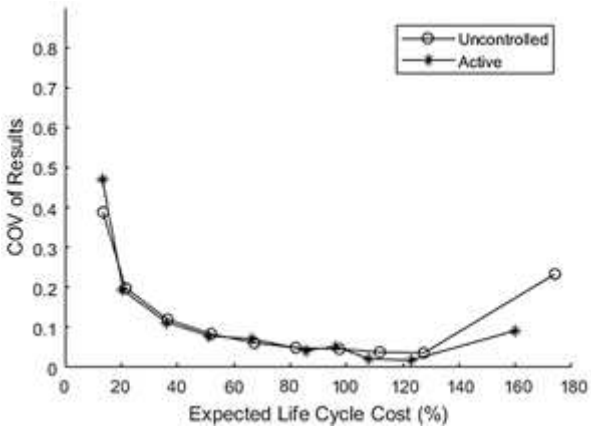


Figure 11

Coefficient of variation of the expected life-cycle damage cost of buildings in Monte-Carlo simulation.

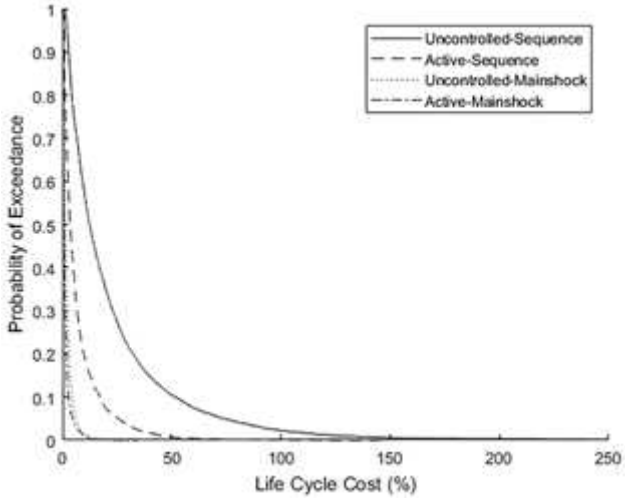


Figure 12

Loss curve of steel moment resisting frame building without and with active vibration control system, located in Tehran metro-city, under any probable future earthquake scenario.

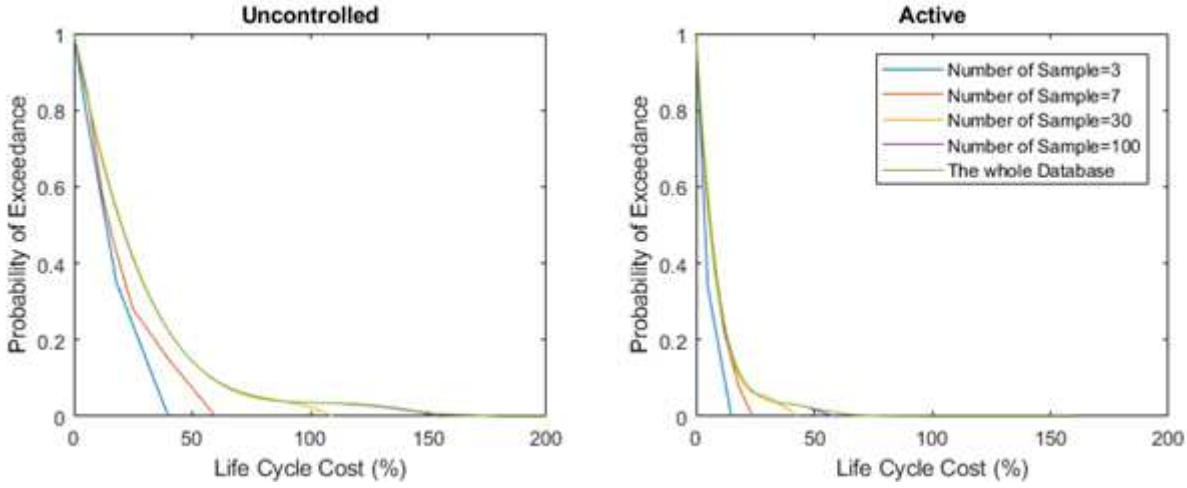


Figure 13

Results of Bootstrapping method for sensitivity evaluation of sampling method to the number of generated samples.

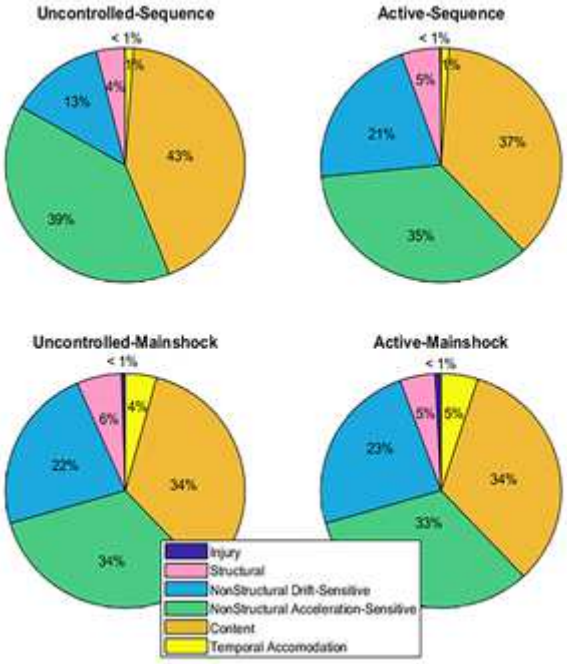


**Figure 14**

Contribution of each damage type in the total damage cost of buildings without and with optimally designed active vibration control system during its lifetime in two different cases of considering and neglecting the aftershock events.

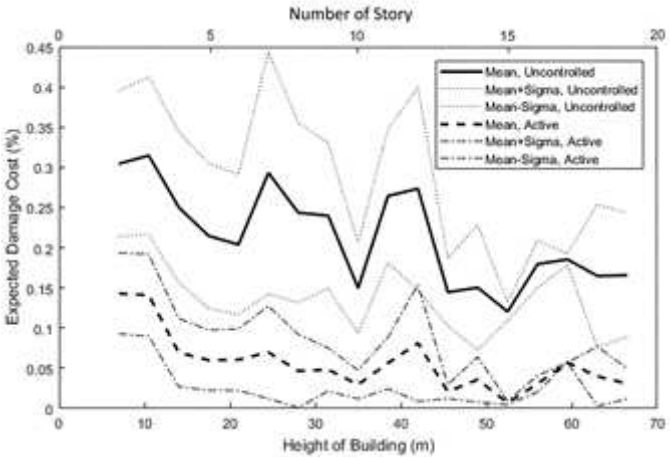


**Figure 15**

Variation of the total building life-cycle damage cost to the height of buildings under earthquake scenarios.

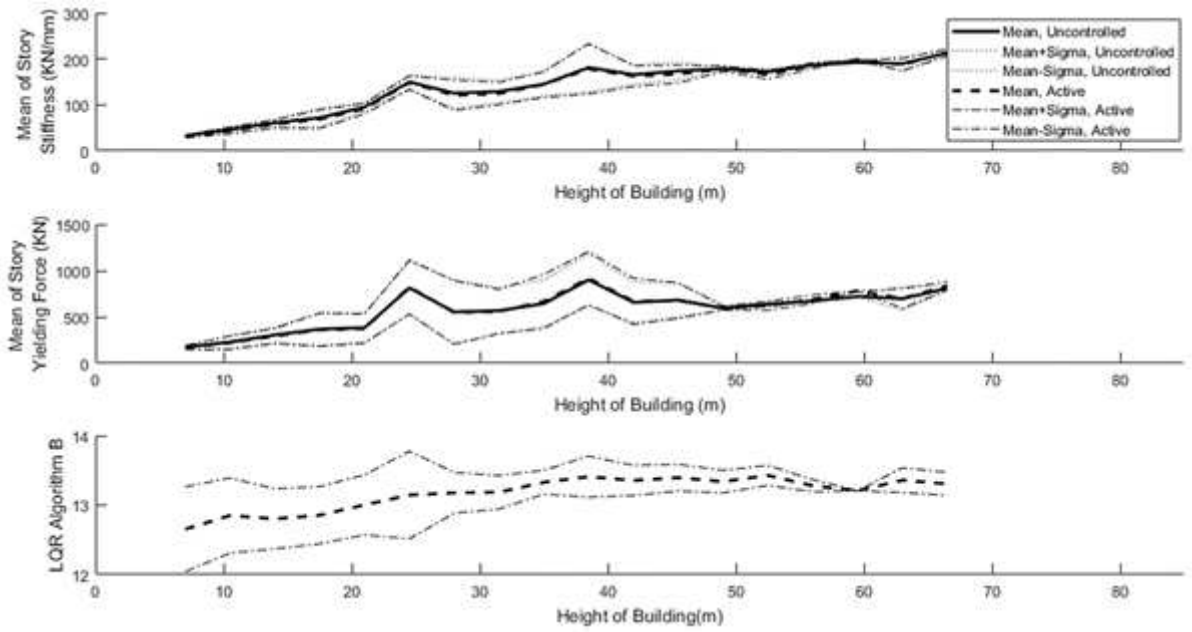


## Figure 16

Variation of building properties (stories stiffness and yielding forces) for both uncontrolled and controlled building as well as optimal β parameter of active LQR algorithm due to building height changes.

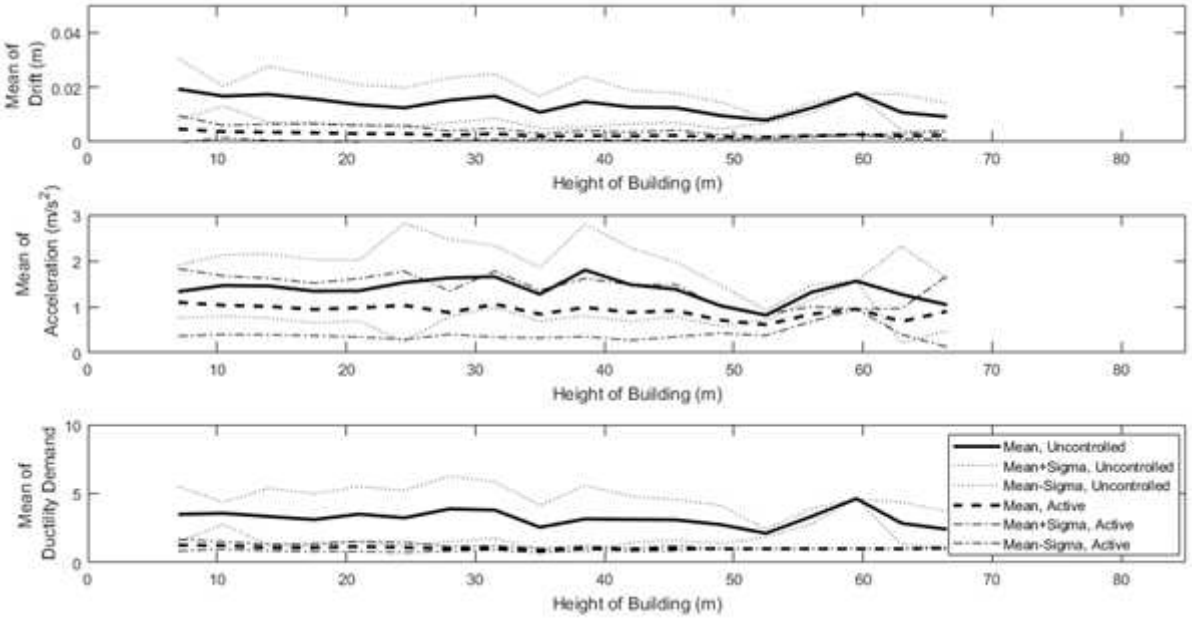


## Figure 17

Variation of the mean value of structural responses of buildings without and with active vibration control system under random earthquake scenarios.

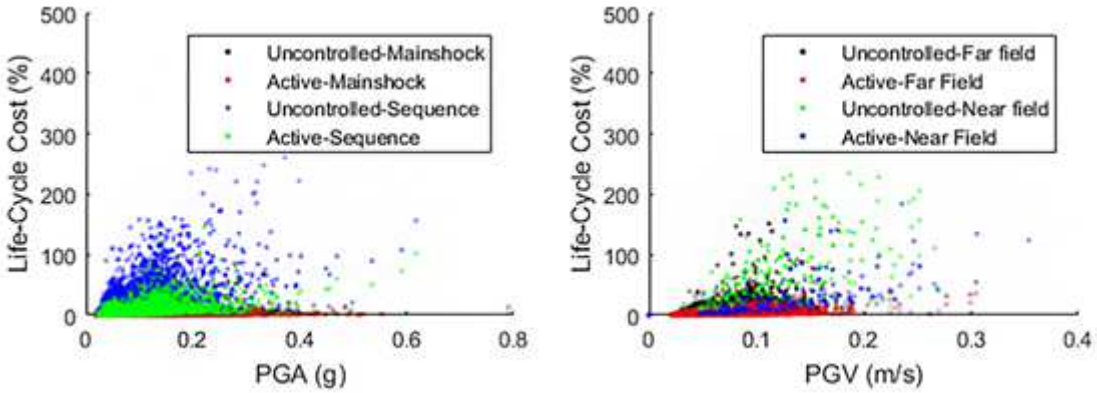


**Figure 18**

Life-cycle damage cost sensitivity to the ground motion parameters (PGA, and PGV).

## Supplementary Files

This is a list of supplementary files associated with this preprint. Click to download.

- Appendix.docx